*Physics – Uspekhi* **49** (7) 667 – 691 (2006) 

*REVIEWS OF TOPICAL PROBLEMS* PACS numbers: **02.40. – k, 11.15. – q, 11.27. + d**, 74.20.De

# Knots and links in the order parameter distributions of strongly correlated systems

A P Protogenov

DOI: 10.1070/PU2006v049n07ABEH006022

## Contents



**Abstract. Research on the coherent distribution of order parameters determining phase existence regions in the two-component Ginzburg – Landau model is reviewed. A major result of this research, obtained by formulating this model in terms of gauged order parameters (the unit vector field n, the density $\rho^2$, and the particle momentum c), is that some of the universal phase and field configuration properties are determined by topological features related to the Hopf invariant $Q$ and its generalizations. For sufficiently low densities, a ring-shaped density distribution may be favored over stripes. For an $L < Q$ phase ($L$ being the mutual linking index of the n and c field configurations), a gain in free energy occurs when a transition to a nonuniform current state occurs. A universal mechanism accounting for decorrelation with increasing charge density is discussed. The second part of the review is concerned with implications of non-Abelian field theory for knotted configurations. The key properties of semiclassical configurations arising in the Yang – Mills theory and the Skyrme model are discussed in detail, and the relation of these configurations to knotted distributions is scrutinized.**

## 1. Introduction

Critical phenomena in low-dimensional strongly correlated systems are characterized by a surprisingly universal cooperative behavior. In copper oxide-based planar systems, this universality manifests itself in the qualitatively similar behavior of compounds representing different classes. A remarkable feature of media in which strong local interactions between particles compete with delocalized excitations is the emergence of quasi-one-dimensional distributions of charge degrees of freedom. Low-dimensional structures in the distribution of charge and spin degrees of freedom sometimes exist in a phase state from which they may pass to a high-temperature superconducting state.

The existence of such a transition allows describing the aforementioned phases in terms of the model that contains competing phase states as specific limit cases. Investigations into general problems of this kind may bring some insights into their understanding based on the Ginzburg – Landau mean-field theory with a properly chosen order parameter. The key issue in such a universal approach is to identify the way in which the order parameter simultaneously encodes the composition and the spatial distribution of charge and spin degrees of freedom in various phase states. The solution to this problem leads to the controlled mean-field theory for strongly interacting systems.

In view of the recent progress in the solution of similar problems in the non-Abelian theory and in condensed-matter physics, it appears reasonable to give preference to the two-component Ginzburg – Landau model. In the electroweak interaction theory, the two-component order parameter has the meaning of the Higgs doublet of the standard model. In neutral systems, the multicomponent order parameter is widely used in describing various phases in the spinor Bose – Einstein condensates. In electron systems with minimally possible values of electron spin, two components of the complex order parameter allow describing orientational and scalar degrees of freedom of electron excitations.

**A P Protogenov** Institute of Applied Physics,
Russian Academy of Sciences,
ul. Ul'yanova 46, 603950 Nizhnii Novgorod, Russian Federation
Tel. (7-8312) 164 899. E-mail: alprot@appl.sci-nnov.ru

Received 26 December 2005
*Uspekhi Fizicheskikh Nauk* **176** (7) 689 – 715 (2006)
Translated by Yu V Morozov; edited by A M Semikhatov

We show in Sections 2–4 that the universal character of the results obtained is to a large extent due to the order parameter dimensionality, which is two in our case. It is only then that the Hopf invariant can be used to classify three-dimensional configurations of the unit vector **n** describing the distribution of spin degrees of freedom in the longwave limit and to correctly consider phases differing in the character of charge delocalization. The Hopf invariant describes the degree of linking or knotting of the one-dimensional filament manifold on which the unit vector field **n** is defined.

The objective of the present review is to discuss recent data pertaining to the problem under consideration that have been obtained in condensed-matter physics and in field theory in the framework of the generalized O(3) sigma-model. After the exact map of the two-component Ginzburg–Landau model, the sigma-model acquires additional Faddeev's terms [1], accounting for the stability of order parameter configurations. We consider the results of those works in which characteristics of the linking or knotting degree of quasi-one-dimensional field configurations were used to describe the universal behavior of strongly correlated systems.

Investigations into the behavior of a tangle of filaments pose a separate problem, drawing attention for several reasons. First, the topological order associated with short-range links exists in the background of the disorder caused by the random localization of separate parts of the system of entangled vortex filaments. Therefore, the properties of a tangle, unlike those of a point-like particle, are determined by the behavior of its fragments in ultraviolet and infrared limits. Because strong local correlations and delocalized modes coexist in the tangle, an interplay of the asymptotic regimes ensures the finite size and energy scale of the quasi-one-dimensional structure.

A section of a three-dimensional tangle by a plane gives rise to a nonuniform two-dimensional distribution of phase states with the regular or random distribution of electron degrees of freedom belonging to the filament core and regions outside it. Such projection is a natural definition of planar phenomena. It may be considered both as a mode of embedding the physics of two-dimensional phenomena into the ambient three-dimensional space and as a realization of planar states existing in the bulk, at the crystal surface. The section results in a self-generating spin-glass state with a well-defined role of the disorder due to the topological phase separation mechanism. The answer to the question of a small parameter in this competition between the phase states depends on the ratio of state phase volumes and is to a large extent determined by the degree of filament packing in the tangle.

Second, a soft medium such as a tangle of linked and knotted filaments is a topical object studied not only in condensed-matter physics [2] but also in molecular biology, e.g., in connection with the problem of DNA supercoiling. When the coupling constant of the sigma-model becomes a function determining the density distribution, the appearance of a configuration in the form of a chiral double helix as a solution of the equations of motion is the general property of the model. In this domain, the working parameter characterized by an ideal configuration of a given knot type [3] proves to be proportional to the degree of filament packing in the tangle.

For convenience, this review is divided into two parts. The first (Sections 2–4) deals with the properties of field configurations in the O(3) sigma-model and their contribution to free energy. The second part (Section 5) expounds selected results obtained in non-Abelian field theory and related to the problems of condensed-matter physics. Technical problems considered in the Appendix clarify some issues touched upon in the preceding sections of this review. In terms of contents, approaches, and applications, the review is based on the data presented earlier in papers on strongly correlated systems [4–9].

## 2. Free energy

The free energy for the two-component gauge-invariant Ginzburg–Landau model is given by

$$F = \int \mathrm{d}^3x \left[ \sum_\alpha \frac{1}{2m_\alpha} \left| \left( \hbar\partial_k + \mathrm{i}\,\frac{2e}{c}\,A_k \right) \Psi_\alpha \right|^2 + \frac{\mathbf{B}^2}{8\pi} + V(\Psi_1, \Psi_2) \right]. \tag{2.1}$$

Expression (2.1) has previously been used to study two-gap superconductivity [10] and problems of high-temperature superconductivity in different contexts [11–15]. The potential energy $V(\Psi_1, \Psi_2)$ consists of the following terms [16]:

$$V(\Psi_1, \Psi_2) = \sum_\alpha \left[ -b_\alpha |\Psi_\alpha|^2 + \frac{d_\alpha}{2} |\Psi_\alpha|^4 \right] + c|\Psi_1|^2|\Psi_2|^2 + f(\Psi_1\Psi_2^* + \text{c.c.}) + h(\Psi_1^2\Psi_2^{*2} + \text{c.c.}). \tag{2.2}$$

Here, $b_\alpha$, $d_\alpha$, $c$, $f$, and $h$ are constants. This part of the free energy may contain additional terms. For example, Ref. [17] discusses implications of the inclusion of the Lifshitz term $\Psi_1\left(\hbar\partial_k + \mathrm{i}(2e/c)A_k\right)\Psi_2^* + \text{c.c.}$ into (2.2) for the description of chiral phases.

Expression (2.2) contains seven degrees of freedom, two of which (the total length $\rho$ of the vector $\Psi_\alpha = \sqrt{2m_\alpha}\,\rho|\chi_\alpha|\exp(\mathrm{i}\phi_\alpha)$, where $|\chi_1|^2 + |\chi_2|^2 = 1$, and the sum of phases $\phi_1 + \phi_2$ of the fields $\Psi_\alpha$) are related to the scalar sector of the theory, while the remaining five (two independent components of the three-dimensional unit vector $n^a = (\sin\vartheta\cos\varphi, \sin\vartheta\sin\varphi, \cos\vartheta)$ and three components of the current density field $\mathbf{a} = \mathrm{i}\left[\chi_1\nabla\chi_1^* - \text{c.c.} + (1 \to 2)\right]$) are the degrees of freedom related to spin orientation. Here, $|\chi_1| = \cos\vartheta/2$, $|\chi_2| = \sin\vartheta/2$, and $\varphi = \phi_1 - \phi_2$. The internal gauge field **A** and its self-energy $(\mathrm{rot}\,\mathbf{A})^2/8\pi$ determine the contribution of charge degrees of freedom. To explicitly distinguish the scalar and orientational degrees of freedom in expression (2.1) for the purpose of description, it is necessary to pass to gauge-invariant variables as proposed in Ref. [10].

### 2.1 Exact map

Reference [10] demonstrated the existence of an exact map of model (2.1) to the extended $(3+0)$-dimensional variant of the nonlinear O(3) sigma-model:

$$F = F_\mathbf{n} + F_\rho + F_\mathbf{c} + F_\mathrm{int} = \int \mathrm{d}^3x \left[ \frac{1}{4}\,\rho^2(\partial_k\mathbf{n})^2 + (\partial_k\rho)^2 + \frac{1}{16}\,\rho^2\mathbf{c}^2 + (F_{ik} - H_{ik})^2 + V(\rho, n_1, n_3) \right]. \tag{2.3}$$

The free energy in (2.3) is given by the scalar $\rho^2$, the unit vector field $n^a = \bar{\chi}\sigma^a\chi$, and the momentum field $\mathbf{c} = \mathbf{J}/\rho^2 = \mathbf{a} - \mathbf{A}$, where the total current **J** contains the

paramagnetic $\left(\mathbf{a} = \mathrm{i}\left[\chi_1 \nabla \chi_1^* - \text{c.c.} + (1 \to 2)\right]\right)$ and diamagnetic $(-\mathbf{A})$ parts. Here, $\bar{\chi} = (\chi_1^*, \chi_2^*)$ and $\sigma^a$ are the Pauli matrices. Expression (2.3) is written with the notation $F_{ik} = \partial_i c_k - \partial_k c_i$ and $H_{ik} = \mathbf{n}\,[\partial_i \mathbf{n} \times \partial_k \mathbf{n}] = \partial_i a_k - \partial_k a_i$, as well as dimensionless units of length $L = (\xi_1 + \xi_2)/2$ with the coherence length $\xi_\alpha = \hbar/\sqrt{2m b_\alpha}$ (in the case of equal masses $m_\alpha = m$) and momentum $\hbar/L$ (as the unit of measure of the momentum $\mathbf{c}$), the unit of particle density $c^2/(512\pi e^2 L^2)$ per unit mass (using parameterization of $\Psi_\alpha$), and the energy unit $\gamma/L$ with $\gamma = (c\hbar/e)^2/512\pi$. Expression (2.3) was obtained in [10] using the gauge-invariant identity

$$|\partial \chi_1|^2 + |\partial \chi_2|^2 - \frac{\mathbf{a}^2}{4} = \frac{1}{4}\,(\partial \mathbf{n})^2$$

and the Mermin–Ho relation [18]

$$(\mathrm{rot}\,\mathbf{a})_i = \frac{1}{2}\,\varepsilon_{ijk} H_{jk}\,.$$

The Ginzburg–Landau functional in (2.3) depends on the gauge-invariant order parameters $\rho^2$, $\mathbf{c}$, and $\mathbf{n}$ that characterize the spatial distribution of electron degrees of freedom with or without a current. The functions $\chi_\alpha$ determine the orientation of the unit vector $\mathbf{n}$ describing the properties of the magnetic order in the longwave limit. Moreover, the functions $\chi_\alpha$ give the paramagnetic component of the current. The kinetic energy density $(1/16)\,\rho^2 \mathbf{c}^2$ and surface energy density $F_{ik}^2$ contribute to the current part $F_\mathbf{c}$ of the free energy. The diamagnetic interaction $-2F_{ik}H_{ik}$ of the fields $\mathbf{a}$ and $\mathbf{c}$ determines the value of energy $F_{\mathrm{int}}$.

Considered formally, the first term on the right-hand side of (2.3) has the form of the Heisenberg antiferromagnetic energy written in the longwave limit. To better understand the role of each term in the free energy and the physical meaning of the components of the two-component order parameter, it is necessary to specify how and which terms of Hamiltonian

$$H = P\left[-t \sum_{\langle ij\rangle,\,\sigma} (c_{i\sigma}^+ c_{j\sigma} + \text{h.c.})\right] P + J \sum_{\langle ij\rangle} \left(\mathbf{S}_i \mathbf{S}_j - \frac{1}{4}\, n_i n_j\right) \quad (2.4)$$

in the $t$–$J$-model (which is standard in studies of various phase states in doped antiferromagnetic dielectrics) determine the physical meaning of variables and the shape of model (2.3). In expression (2.4), $\mathbf{S}_i = c_{i\alpha}^+ \boldsymbol{\sigma}_{\alpha\beta} c_{i\beta}/2$, $n_{i,\sigma} = c_{i\sigma}^+ c_{i\sigma}$, and $P = \prod_i (1 - n_{i,\uparrow} n_{i,\downarrow})$. Elimination of the states doubly occupied at the sites and having oppositely oriented spins from the Hilbert state space with the help of a Gutzwiller projector $P$ converts the kinetic energy in (2.4) to a term essentially different from the trivial kinetic term quadratic in fermion operators in the Fermi systems. From the standpoint of the mean-field theory [9] formulated in terms of paired correlation functions of operators $\psi_\alpha$ and $h_i$, the factorization $c_{i\sigma} = h_i^+ \psi_{i\sigma}$ of the charge and spin degrees of freedom of the electron operator $c_{i\sigma}$, involving the SU(2)-doublets

$$\psi_\uparrow = \begin{pmatrix} f_\uparrow \\ f_\downarrow^+ \end{pmatrix}, \qquad \psi_\downarrow = \begin{pmatrix} f_\downarrow \\ -f_\uparrow^+ \end{pmatrix}, \quad \text{and} \quad h = \begin{pmatrix} h_1 \\ h_2 \end{pmatrix},$$

implies that both the correlation function $\chi_{ij} = \sum_\sigma \langle f_{i\sigma}^+ f_{j\sigma}\rangle$ describing hopping between sites $i$ and $j$ and the correlation function $\Delta_{ij} = \langle f_{i\uparrow} f_{j\downarrow} - f_{i\downarrow} f_{j\uparrow}\rangle$ describing pairing are to be found from two mutually dependent self-consistency equations [19]. These correlation functions determine the contribution of the two terms under the square root in the expression

$$E_\mathbf{k} = \sqrt{\xi_\mathbf{k}^2 + \Delta_\mathbf{k}^2}$$

for the excitation spectrum. This is the distinction from the classical Bardin–Cooper–Schrieffer (BCS) theory in which the part coupled to $\xi_\mathbf{k}$ is assumed to be known. In (2.3), the unit vector $\mathbf{n} = \bar{\chi}\boldsymbol{\sigma}\chi$ directed toward a certain arbitrary point describes the relation between the hopping-related correlations and those determined by pairing the electron degrees of freedom.

The SU(2)-symmetric matrix variable

$$U_{ij} = \begin{pmatrix} -\chi_{ij}^+ & \Delta_{ij}^* \\ \Delta_{ij} & \chi_{ij} \end{pmatrix} = U_{ij}^{\mathrm{d(sf)}} \exp\left(\mathrm{i}\mathbf{a}_{ij}\boldsymbol{\sigma}\right)$$

of the gauge theory of strong correlations [9] is determined by the distribution of hopping and pairing amplitudes $U_{ij}^{\mathrm{d(sf)}}$ in the d-symmetric superconducting $(U_{ij}^{\mathrm{d}})$ state and in the U(1)-symmetric phase with a checkered order of gauge field fluxes $\mathbf{a}_{ij}$ through an elementary cell $(U_{ij}^{\mathrm{sf}})$. We assume, for the purpose of analysis in the present review, that the original state is the phase state with alternating circulation of the U(1)-gauge field $\mathbf{a}_{ij}$. A more complicated analysis of the SU(2) symmetric phase [9] with a gauge field flux equaling $\pi$ (see Section 5) is based on the effective Lagrangian $\mathcal{L}_{\mathrm{SU(2)}} = (1/g^2)\,\mathrm{Tr}\,\mathbf{F}_{\mu\nu}^2$ of the Yang–Mills theory that emerges after integration over fermions $\psi_{i\sigma}$.

It is worth noting that the two-component order parameter in the Ginzburg–Landau functional also arises in the theory with repulsion between particles [20] if the momentum space contains mirror nesting and the integral operator in the self-consistency equation for the anomalous correlation function has one negative eigenvalue (of the two possible ones). In this case, the emergence of quasistationary delocalized states in addition to the bound state suggests the possibility of a phase state in which these modes cannot be disregarded and which undergoes strong fluctuations in the kinetic term in the energy. In the approach under consideration (see also Ref. [20]), the essentially nonuniform distribution of the phase states is due to antiferromagnetically correlated circulations of orbital currents with a large total momentum of fermion pairs. Hence, this distinguishes the Cooper pairs with their zero total momentum from the Fulde–Ferrel–Larkin–Ovchinnikov state, in which excitations have a small total momentum.

The self-energy $H_{ik}^2$ of the internal magnetic field $H_i = 1/2\,\varepsilon_{iks} H_{ks}$ in the longwave limit is proportional to the squared mean value $\langle 0|\mathbf{S}_1[\mathbf{S}_2 \times \mathbf{S}_3]|0\rangle$ of the degree of spin noncollinearity on three sites of a square lattice. The magnetic field appears as a result of the electron removal from the fourth site of certain elementary cells into the dopant reservoir. The arising chiral distributions of spin degrees of freedom are of basic importance for the formation of quasi-one-dimensional spin and charge structures considered in Sections 3 and 4. In the general case, the contribution of such structures to the free energy depends on the term $(H_{ik} - F_{ik})^2$ containing the cross term $-2H_{ik}F_{ik}$ responsible for the coupling between currents $\mathbf{a}$ and $\mathbf{c}$.

Modulation of the exchange integral given by the scalar field $\rho(x, y, z)$ and describing the spin stiffness $\rho^2$ in (2.3) depends on the degree of doping. Indeed, the spin stiffness $\rho^2$ in the mean-field approximation is related to the density $\rho_{\mathrm{h}}^2$ of

positively charged vacant sites as $\rho^2 + \rho_h^2 = 1$ [21]. In the U(1) and SU(2) theories of doped Mott dielectrics, this relation for the operators of charged spinless bosons and neutral fermions with spin 1/2 is discussed in Ref. [9].

The energy densities $H_{ik}^2$ and $F_{ik}^2$ are localized at the boundaries of regions with a nonzero spin density. If $\rho^2 \lesssim 1$, then the hole density $\rho_h^2$ exists in a space complementary to the spin density definition space. Bearing this in mind, as well as the structure of the distribution of spin degrees of freedom on the lattice (see Fig. 4 in Ref. [5, p. 14]), the authors of Ref. [22] proposed a low-dimensional analog of the holography principle. Its application in planar systems leads to the conclusion that the distribution of states with the destroyed antiferromagnetic order has a quasi-one-dimensional boundary character.

Expression (2.3) is convenient for the analysis of different phase states on the 'doping level – temperature' phase diagram. Based on configurations of the field **n**, it is possible to specify [9] the mean-field theories for phases with well-developed quantum fluctuations. Therefore, in what follows, we use this equation for the free energy as a base, because it is most suitable for the description of distributions of charge and spin degrees of freedom. The spin sector of the theory is described with the help of the $CP^1$-representation of the nonlinear O(3) sigma-model in the form similar to Ginzburg – Landau functional (2.1). It follows from the comparison of different forms in which the Ginzburg – Landau model is represented [9] that vortex configurations of the fields $\Psi_\alpha$ in model (2.1) are equivalent to the **n** field textures in terms of model (2.3). It is equally worth noting that the ansatz used for the components of $\Psi_\alpha$ involves factorization of the longitudinal $\rho$ and transverse $\chi_\alpha$ degrees of freedom. In a superconducting state, an important role is played by the composition of spin and charge degrees of freedom.

### 2.2 Possible phase states

In a soft variant, $\rho \neq \text{const}$, of the extended **n**-field model (2.3), the factors in the first term on the right-hand side of the equation describe the influence of the distribution of spin stiffness $\rho^2$ on the **n** field configurations and the distribution of the square $(\partial_k \mathbf{n})^2$ of the inverse characteristic length of variation of the spin density field on the $\rho$ field configurations. The character of the effect of the field **c** on the configurations of **n** and $\rho$ is apparent from the equations of motion

$$[\mathbf{n} \times \Delta \mathbf{n}] + \frac{2}{\rho}(\partial_k \rho)[\mathbf{n} \times \partial_k \mathbf{n}] + \frac{8}{\rho^2}(\partial_i H_{ik})(\partial_k \mathbf{n}) - \frac{2}{\rho^2} F_{ik}[\partial_i \mathbf{n} \times \partial_k \mathbf{n}] + \frac{4}{\rho^2}\,\partial_i\{F_{ik}[\mathbf{n} \times \partial_k \mathbf{n}]\} = 0\,, \quad (2.5)$$

$$\Delta\rho + \left[b - \frac{1}{4}(\partial_k \mathbf{n})^2 - \frac{1}{16}\,\mathbf{c}^2\right]\rho - d\rho^3 = 0\,, \quad (2.6)$$

$$\partial_k F_{ki} - \partial_k H_{ki} - \frac{\rho^2}{32}\,c_i = 0\,. \quad (2.7)$$

For simplicity, Eqns (2.5) – (2.7) were written under the assumption that the potential energy is $V = -b\rho^2 + (d/2)\rho^4$.

It follows from Eqns (2.5) – (2.7) that competition between the order parameters $\rho$, **n**, and **c** may be a cause of the coexistence of phase states with different ordering of charge and spin degrees of freedom. Listed below are the limit cases of model (2.3) in inhomogeneous ($\mathbf{n} \neq \text{const}$) situations:

(1) A state with $\mathbf{n} \neq \text{const}$, $\mathbf{c} = 0$, and $\rho = \text{const}$.

(2) A state in the case of a quasi-one-dimensional distribution of the density $\rho^2$ with $\mathbf{c} = 0$.

(3) An inhomogeneous superconducting state with $\mathbf{c} \neq 0$ and $\rho = \text{const}$.

(4) The general case: all order parameters are present and $\rho \neq \text{const}$.

The case where $\mathbf{n} = \text{const}$, $\mathbf{c} \neq 0$, and $\rho \neq \text{const}$ corresponds to the classical one-component Ginzburg – Landau model with the external magnetic field potential **A**.

The above states have been considered in recent publications. Each item of the foregoing list is discussed in detail in Section 3.

## 3. Free-energy bounds

### 3.1 The Skyrme – Faddeev model

We consider the first case listed in Section 2.2. In this limit, the free energy is

$$F = \int \mathrm{d}^3x \left[g_1(\partial_k \mathbf{n})^2 + g_2\left(\mathbf{n}\,[\partial_i \mathbf{n} \times \partial_k \mathbf{n}]\right)^2\right]. \quad (3.1)$$

We assumed that the constant value of $\rho = \rho_0$ in the phase of interest can be found from the minimum of the potential $V$ and introduced the notation $g_i$ for the coupling constant. The properties of model (3.1) are studied in detail in Refs [23 – 39].

It is easy to see, by substituting $x \to x/R$, that the first term in Eqn (3.1) is proportional to the characteristic size $R$ of the **n** field configurations, while the second term is inversely proportional to this scale (this conclusion is to be clarified in Sections 3.2 and 4.1 – 4.4). Therefore, the energy in (3.1) has a minimum equal to $2\sqrt{g_1 g_2}$ and achievable at $R = \sqrt{g_2/g_1}$.

Thus, the finite value of the energy and the spatial scale of a tangle of filaments are given by its ultraviolet characteristic, i.e., the coupling constant $g_2$. This explains why the second term in model (3.1) allows obviating Derrick's ban [30] on the existence of three-dimensional static configurations of a finite size. In the absence of this term, the minimum free energy value corresponds to the field configuration with $R \to 0$. As noted in Section 2.1, this three-particle term characterizes, in the longwave limit, the average degree of noncollinearity $\langle 0|\mathbf{S}_1\,[\mathbf{S}_2 \times \mathbf{S}_3]|0\rangle$ in the orientation of three spins located in the sites of a cell in a square lattice.

It was shown in Refs [27 – 29] that the lower energy bound in model (3.1),

$$F \geqslant 32\pi^2\,|Q|^{3/4}\,, \quad (3.2)$$

is determined by the Hopf invariant [31, 32]

$$Q = \frac{1}{16\pi^2}\int \mathrm{d}^3x\,\varepsilon_{ikl}\,a_i \partial_k a_l = \frac{1}{8\pi^2}\int \mathrm{d}^3x\;\mathbf{a}\,[\nabla \times \mathbf{a}]\,. \quad (3.3)$$

We recall that the gauge potential $a_i$ in expression (3.3) parameterizes the average degree of noncollinearity of the orientations of the neighboring spins as $H_{ik} = \mathbf{n}\,[\partial_i \mathbf{n} \times \partial_k \mathbf{n}] \equiv \partial_i a_k - \partial_k a_i$. The fact that $F_{\min} \sim |Q|^\alpha$ at $\alpha = 3/4 < 1$ implies stability of configurations with a larger $Q$ value with respect to the decay into distributions with smaller values of the Hopf invariant. A detailed analysis of the problem for large $Q$ values can be found in Ref. [33].

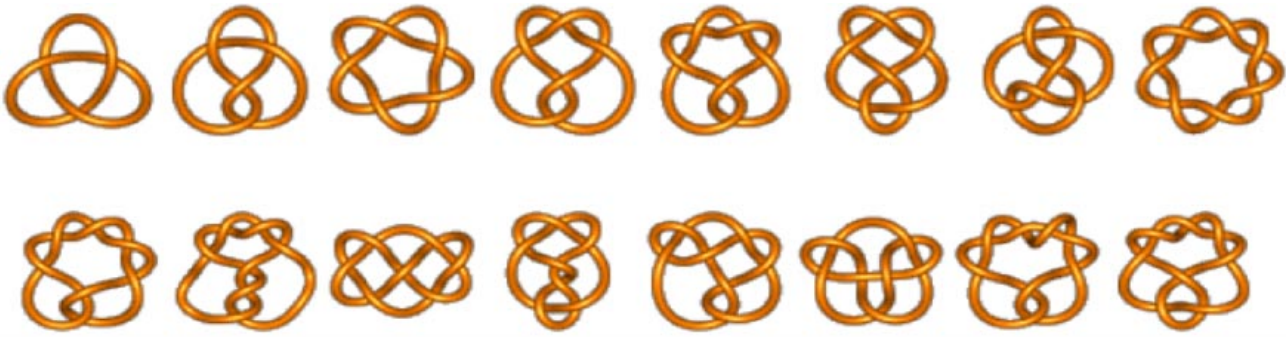

**Figure 1.** Examples of the simplest knotted configurations.

The dependence $F_{\min} \sim |Q|^{3/4}$ in (3.3) with the use of the boundary condition $\mathbf{n} = (0, 0, 1)$ at spatial infinity was confirmed in Refs [24–26] by numerical calculations of the **n** field configurations. Such a boundary condition means that the space $\mathsf{R}^3$ of the **n** field definition is effectively compactified into a three-dimensional sphere $\mathsf{S}^3$. Thereby, the unit vector field **n** maps the sphere $\mathsf{S}^3$ into the space of its values belonging to a two-dimensional sphere $\mathsf{S}^2$.

Let the vector **n** be directed toward a certain arbitrary point of the two-dimensional sphere. What is then the pre-image of this point in $\mathsf{S}^3$? In other words, what manifold of points from the vector $\mathbf{n}(x, y, z)$ definition domain contributes to the span of **n** at the two-dimensional sphere? The space $\mathsf{S}^3$ being compact and one dimension larger than the sphere $\mathsf{S}^2$, the pre-images of points on $\mathsf{S}^2$ are closed and, generally speaking, linked lines on $\mathsf{S}^3$. The integer $Q$ cannot define the degree of the map because the basic and target spaces are of different dimensions. The Hopf invariant $Q$ in (3.3) describes the complexity of the linking and knotting of lines in the sphere $\mathsf{S}^3$. It belongs to the set of integers $\mathsf{Z}$, equal to the homotopy group under consideration, $\pi_3(\mathsf{S}^2) = \mathsf{Z}$. Specifically, $Q = 1$ for two singly linked circles, $Q = 6$ for one of the simplest knots (trefoil), etc. (Fig. 1).

Problems pertaining to the knot theory and its numerous applications are extensively discussed in the literature [34, 35] as well as in web resources [36–42]. The interested reader is referred to these publications.

We note that the Hopf invariant cannot be written as the integral of a density local in the field **n**. The integrand depends on the potential $a$ and the gauge field strength $H$. In terms of differential geometry, the Hopf invariant can be written as

$$Q \sim \int_{\mathsf{S}^3} H \wedge a \,.$$

Moreover, the 2-form $H$ is exact by virtue of the triviality $(H^2(\mathsf{S}^3) = 0)$ of the second cohomology group of $\mathsf{S}^3$. This means that it can always be expressed through the potential as $H = \mathrm{d}a$.

To summarize, all **n** field configurations are categorized into classes by Hopf invariant values that, in turn, determine the hierarchy of local free energy minima, in accordance with relation (3.2). It is worth mentioning that linked and knotted configurations can be enumerated with the help of the Hopf invariant only in the case of the coset space $\mathrm{SU}(2)/\mathrm{U}(1) = \mathrm{CP}^1 = \mathsf{S}^2$ because the homotopy group $\pi_3(\mathrm{CP}^M) = 0$ is trivial for $M > 1$ [43].

### 3.2 Current states

We consider the distributions of fields with a nonzero current **J** assuming that $\rho = \mathrm{const}$. In this case, the free energy has the form

$$F = F_{\mathbf{n}} + F_{\mathbf{c}} + F_{\mathrm{int}} = \int \mathrm{d}^3x \left\{ \left[ (\partial_k \mathbf{n})^2 + H_{ik}^2 \right] + \left( \frac{1}{4}\,\mathbf{c}^2 + F_{ik}^2 \right) - 2F_{ik}H_{ik} \right\}. \tag{3.4}$$

The minus sign in the interaction energy $F_{\mathrm{int}}$ of the fields **c** and **n** reflects the diamagnetism ($\mathbf{c} = \mathbf{a} - \mathbf{A}$) of the state being considered. Because of this interaction, the coupling constant $g_2$ at the $H_{ik}^2$ term in model (3.1), normalized to unity in expression (3.4), effectively decreases due to the competition between the **a** and **c** currents such that the state with momentum $\mathbf{c} \neq 0$ has a smaller energy than its minimal value in inequality (3.2).

The exact lower bound of the free energy in a state with $\mathbf{c} \neq 0$ can be found using the auxiliary inequality

$$F_{\mathbf{n}}^{5/6} F_{\mathbf{c}}^{1/2} \geqslant (32\pi^2)^{4/3} |L| \,, \tag{3.5}$$

where the number

$$L = \frac{1}{16\pi^2} \int \mathrm{d}^3x\, \varepsilon_{ikl}\, c_i\, \partial_k a_l \tag{3.6}$$

defines the degree of mutual linking [44–47] of current lines and lines of the magnetic field $\mathbf{H} = [\nabla \times \mathbf{a}]$. The proof of inequality (3.5) is presented in the Appendix. The mutual linking index $L$, similarly to $Q$, is an integral of motion [45, 47] in the barotropic state.

The Hopf invariant $Q$ and the mutual linking index $L$ are matrix elements of the symmetric matrix [44]

$$K_{\alpha\beta} = \frac{1}{16\pi^2} \int \mathrm{d}^3x\, \varepsilon_{ikl}\, a_i^{\alpha}\, \partial_k a_l^{\beta} = \begin{pmatrix} Q & L' \\ L & Q' \end{pmatrix}, \tag{3.7}$$

which characterizes link-based configurations of the spin and charge degrees of freedom. In this matrix ($L = L'$) at $a_i^1 \equiv a_i$ and $a_i^2 \equiv c_i$, the integral can also be defined by the asymptotic linking number [44].

One fact essential for further discussion deserves attention. The vector of momentum $\mathbf{c} = \mathbf{J}/\rho^2$ normalized by the density, unlike the unit vector **n**, belongs to a noncompact manifold. As a result, the Hopf numbers defined with its help in (3.7) are not, generally speaking, integers: $L, Q' \notin \mathsf{Z}$. In a superconducting current state where the Abelian U(1) gauge symmetry is broken and the charge is not conserved, the

numbers $L$ and $Q'$ play the role of continuous interpolation parameters connecting the compressible and incompressible ($K_{\alpha\beta} \in \mathbf{Z}$) phases. From this standpoint, the superconducting states with $K_{\alpha\beta} \in \mathbf{Z}$ and $K_{\alpha\beta} \notin \mathbf{Z}$ belong to the same universality class [48].

The search for the lower bound of function (3.5) is based on the Schwartz – Cauchy – Bunyakovskii inequality, in addition to inequality (3.5):

$$F_{\text{int}} \leqslant 2\|F_{ik}\|_2 \times \|H_{ik}\|_2 \leqslant 2F_{\mathbf{c}}^{1/2}F_{\mathbf{n}}^{1/2}\,. \tag{3.8}$$

Here, $\|F_{ik}\|_2 \equiv [\int \mathrm{d}^3x\, F_{ik}^2]^{1/2}$. We note that the equality on the right-hand side of (3.8) is achieved in the ultraviolet limit, when the size of linked vortex configurations is sufficiently small. Substitution of the boundary value of $F_{\text{int}}$ in Eqn (3.4) yields

$$F \geqslant F_{\min} = (F_{\mathbf{n}}^{1/2} - F_{\mathbf{c}}^{1/2})^2\,. \tag{3.9}$$

The Hopf configuration with $Q = 1$, at which the lower limit is achieved in inequality (3.2), has the form of two linked rings with radii $R$ [49] and $(F_{\mathbf{n}})_{\min} = 2\pi^2R^3(8/R^2 + 8/R^4)\big|_{R=1} = 32\pi^2$. In our case, with $\mathbf{c} \neq 0$, it is also assumed that there are configurations for which the equality in (3.5) holds.

One more important fact also deserving attention is to be discussed at greater length in Section 4.1. At small $\rho$, and hence at large $\mathbf{c}$ field values (all quantities entering (3.5) being of the same order), one is faced with instability of linked configurations with respect to relatively small deviations; this puts restriction on $F_{\mathbf{c}}$ values from above.

Taking this into account, the substitution of relation $F_{\mathbf{c}}^{1/2} = (32\pi^2)^{4/3}\,F_{\mathbf{n}}^{-5/6}\,|L|$ for the lower bound of $F_{\mathbf{c}}$ and $F_{\mathbf{n}} = 32\pi^2\,|Q|^{3/4}$ in the right-hand side of (3.9) yields, for states with $Q \neq 0$,

$$F \geqslant 32\pi^2\,|Q|^{3/4}\left(1 - \frac{|L|}{|Q|}\right)^2\,. \tag{3.10}$$

It follows from relation (3.10) that for all numbers $L < Q$, the ground state energy is smaller than in model (3.1) for which inequality (3.2) holds. The case of the energy decrease can be understood from the comparison of quantities entering expression (3.4). Even in the presence of a large paramagnetic contribution of $\mathbf{a}$ to the current $\mathbf{J}$, the diamagnetic interaction in a superconducting state for all classes of states with $L < Q$ results in decreasing the current self-energy $F_{\mathbf{c}}$ and part of the energy $F_{\mathbf{n}}$ associated with the field $\mathbf{n}$ dynamics. In the state under consideration, the total momentum $\mathbf{c}$ does not vanish. In this respect, an inhomogeneous state with a current is analogous to the state proposed in Refs [50, 51]. We note, however, that this analogy is limited because the Ginzburg – Landau functional for the Larkin-Ovchinnikov – Fulde – Ferrel state is different [52, 53] from the initial state in this review, despite the presence of higher derivatives.

## 4. Phase state properties

### 4.1 Stability of knots

We consider the problem of stability [29] of the standard Hopf map $\mathbf{S}^3 \to \mathbf{S}^2$ at $Q = 1$:

$$\mathbf{n}\,\boldsymbol{\sigma} = \psi^+\sigma_3\,\psi\,, \tag{4.1}$$

where

$$\psi = (1 - \mathrm{i}\mathbf{r}\boldsymbol{\sigma})(1 + \mathrm{i}\mathbf{r}\boldsymbol{\sigma})^{-1}\,. \tag{4.2}$$

In the toroidal system of coordinates,

$$x + \mathrm{i}y = \frac{\sinh u}{\cosh u + \cos\beta}\exp(\mathrm{i}\alpha)\,, \qquad z = \frac{\sin\alpha}{\cosh u + \cos\beta}\,,$$
$$0 \leqslant u < \infty\,, \qquad 0 < \alpha < 2\pi\,, \qquad 0 < \beta < 2\pi\,, \tag{4.3}$$

$$\tan\frac{n_1}{n_2} = \alpha - \beta\,, \qquad n_3 = 1 - 2\tanh u\,. \tag{4.4}$$

It follows from the above expressions [54] that the entire space is stratified into tori $u = \text{const}$, and any vortex line winds one coil around a torus at $Q = 1$.

In the case of an arbitrary $Q$ value, the Hopf map $\Phi$ can be described as follows. Let an arbitrary point on the sphere $\mathbf{S}^3$ correspond to a pair of complex numbers $(z^0, z^1)$ satisfying the condition $z^a\bar{z}_a = 1$, where $\bar{z}_0 = \bar{z}^0$ and $\bar{z}_1 = \bar{z}^1$. The Hopf map defines the correspondence between this point (more precisely, between points at a three-dimensional sphere localized on a closed curve) and a point from the space $\mathrm{CP}^1 = \mathbf{S}^2$ with homogeneous coordinates $z^0, z^1$. The energy of such a map $\Phi$ on the sphere $\mathbf{S}^3$ with radius $R$ is constant; it is $F = 16\pi^2(R + R^{-1}) \geqslant 32\pi^2$ at $Q = 1$.

Both terms in the last expression are stationary under field variations. In other words, $\Phi$ is a solution of the equations of motion at all values of the radius $R$. Generally speaking, the bound for the free energy from below indicates that the solution may be unstable at a sufficiently large scale of $R$. Because the instability of knotted $\mathbf{n}$-field configurations at large enough $R$ is of primary importance for the further discussion, it needs to be considered at greater length.

The energy $F[\Phi + \delta\Phi]$ for the Hopf map $\Phi + \delta\Phi$ is expressed as

$$F[\Phi + \delta\Phi] = F[\Phi] + \int_M \mathrm{d}^3x\, E[\delta\Phi, \partial_i\delta\Phi]\,,$$

where $E[\delta\Phi, \partial_i\delta\Phi]$ is a function that is quadratic in its arguments and the domain $M$ in the present case corresponds to a sphere. We are interested in the possibility of negative eigenvalues of the quadratic form $\delta F = \int_M \mathrm{d}^3x\, E[\delta\Phi, \partial_i\delta\Phi]$.

The variables $z^a$ are transformed under the action of operators from the fundamental representation of the group U(2). The Hopf map $\Phi$ is invariant under the U(2) action in the sense that $\Phi(z^a)$ and $\Phi(U_b^a z^b)$ are equivalent under SO(3)-transformations of the target space $\mathbf{S}^2$. This means that the group U(2) also acts in the target space of $\Phi$; in other words, it acts in the space of perturbations $\delta\Phi$, too. Therefore, it is possible to decompose the space of perturbations into irreducible representations of U(2) and consider the perturbation as specified below.

The perturbed field maps $z^a$ into a point of $\mathrm{CP}^1$ with homogeneous coordinates $z^a + \theta^a$, where

$$\theta^a = T_{mn\ldots r}^{ab\ldots d}\,\bar{z}_b \ldots \bar{z}_d\, z^m \ldots z^r\,,$$

and $T_{mn\ldots r}^{ab\ldots d}$ is a constant infinitesimal tensor. In terms of the unit vector $\mathbf{n}(z^a, \bar{z}_a)$, the Hopf map $\Phi$ is expressed as

$$n_1 + n_2 = 2z^0\,\bar{z}_1\,,$$

$$n_3 = z^1\,\bar{z}_1 - z^0\,\bar{z}_0\,,$$

and the perturbations being considered are $\delta n_a(z^a, \bar{z}_a)$, where

$$\delta n_1 + \mathrm{i}\delta n_2 = 2(\bar{z}_1)^2\omega - 2(z^0)^2\bar{\omega}\,,$$

$$\delta n_3 = -2\bar{z}_0\bar{z}_1\omega - 2z^0z^1\bar{\omega}\,,$$

with $\omega = \bar{z}\theta^0 - z^0\theta^1$.

For a few first modes, the energy variations $\delta F$ are as follows:

(1) If $\theta^a = t^a$ is constant, then $\delta F = 4\pi^2(t^a\bar{t}_a)(2/R - R)$. These modes are 'positive' at $R < \sqrt{2}$ and negative at $R > \sqrt{2}$. In other words, the Hopf map is actually unstable for $R > \sqrt{2}$.

(2) If $\theta^a$ is $t^{ab}\bar{z}_b$ and the matrix $t^{ab}$ is asymmetric, then $\delta F = 0$, i.e., the mode vanishes.

(3) If $\theta^a = t^a_m z^m$ at $t^a_a = 0$ and $\bar{t}^a_m = t^a_m$, then $\delta F = 128\pi^2(t^b_a\bar{t}^a_b)/(3R)$. Such perturbations are positive at any $R$.

Thus, perturbation of the Hopf map contains a negative mode at $R > \sqrt{2}$.

We consider a one-parameter family of configurations with $Q = 1$ containing the Hopf map and one of the negative modes. Geometrically, this family of fields $\Phi_\lambda$ with a positive parameter $\lambda$ can be described as follows [29]. Let the stereographic projection $\mathsf{S}^3 \to \mathsf{R}^3$ be denoted by $P$ and the dilation operation in $\mathsf{R}^3$ with a constant scale factor $\lambda > 0$ by $\mathrm{D}_\lambda$. The family of fields $\Phi_\lambda$ is defined as $\Phi_\lambda := \Phi \circ P^{-1} \circ \mathrm{D}_\lambda \circ P$. The energy of these fields is

$$F_\lambda[\Phi_\lambda] = \frac{64\pi^2\lambda R}{(\lambda+1)^2} + \frac{8\pi^2(\lambda^2+1)}{\lambda R}\,.$$

At $\lambda = 1$, the result is known: $F_1 = 16\pi^2(R + R^{-1})$.

It follows from the calculation of the $\lambda$ value at which the energy $F_\lambda[\Phi_\lambda]$ has a minimum that at $R < \sqrt{2}$, this minimum exists in the Hopf map with $\lambda = 1$. If $R > \sqrt{2}$, the minimum of $F_\lambda[\Phi_\lambda]$ is achieved when $\lambda$ is one of the roots in the equation

$$\lambda^2 + 2(1 - \sqrt{2}\,R)\lambda + 1 = 0\,.$$

In this case, the minimum energy is $F_{\lambda\,\min} = 32\sqrt{2}\,\pi^2 - 16\pi^2/R$. This solution is not distributed over the entire space $\mathsf{S}^3$; rather, it is localized in the vicinity of a certain distinguished point, i.e., the basic point of the stereographic projection. In the limit as $R \to \infty$, there are configurations with the energy $F_{\min}(R \to \infty) = 32\sqrt{2}\,\pi^2$ and $Q = 1$ in the $\mathsf{R}^3$ space. These configurations consist of the inverse $P^{-1}$-stereographic projection $\mathsf{R}^3 \to \mathsf{S}^3$ and the subsequent Hopf map $\Phi$.

As an example of configurations with $Q \geqslant 1$, we consider fields that map $(z^0, z^1)$ into a point having the homogeneous coordinates $[(z^0)^m/|z^0|^{m-1}, (z^1)^n/|z^1|^{n-1}]$. For the Hopf map, $m = 1$, $n = 1$. For $m > 1$, $n > 1$, the Hopf invariant and the energy [29] are

$$Q = mn\,,$$

$$F = 8\pi^2 R + 4\pi^2(m^2+n^2)\left(R + \frac{2}{R}\right).$$

Minimization of the energy $F$ with respect to the radius $R$ yields

$$F_{\min} = 8\pi^2\sqrt{2(m^2+n^2)(2+m^2+n^2)}$$

with

$$R = \left(\frac{2}{1 + 2/(m^2+n^2)}\right)^{1/2}.$$

The last expression indicates that the characteristic size of an optimum configuration with $Q > 1$ is somewhat enlarged, because it lies in the interval $1 < R < \sqrt{2}$.

### 4.2 Density as a coupling constant

A state with perturbed antiferromagnetic order at the boundary of regions where $(\partial_k\rho)^2 \neq 0$ makes up a background for the transition to an inhomogeneous superconducting phase with $F_{ik} \neq 0$. Properties of this transition at a varying density $\rho^2$ are convenient to discuss starting from a superconducting state with $\rho = \mathrm{const}$. In this phase, the characteristic density value $\rho_0^2$ plays the role of the governing parameter of the system.

Let the parameter $\rho$ vary over a certain interval. All the terms in expression (2.3) being of the same order, an increase in $\rho_0$ leads to a decrease in the momentum $\mathbf{c}$, and hence of the mutual linking index $L$. Increasing $\rho_0$ indicates that the concentration of vacancies or the so-called holes decreases. In this case, the gain of the free energy in (3.10) also decreases at a sufficiently small $L$ and large $32\pi^2|Q|^{3/4}$.

As $\rho_0$ decreases, the following effect emerges. The radius $\mathcal{R}$ of the compactification $\mathsf{R}^3 \to \mathsf{S}^3$, proportional to $R \sim g_1^{-1/2} \sim \rho_0^{-1}$ [see (2.3) and the discussion after (3.1)], increases until it exceeds a certain critical value $R_{\mathrm{cr}}$. As shown in Section 4.1, the Hopf map at $\mathcal{R} > R_{\mathrm{cr}} = \sqrt{2}$ is unstable [29] with respect to relatively small perturbations of linked field configurations. Hence, there is a spontaneous violation of the U(2) symmetry associated with the Hopf map. This means that the topological $\mathbf{n}$ and $\mathbf{c}$ field configurations are not distributed over the entire $\mathsf{S}^3$ space; instead, they are concentrated near a certain point (the base point of the stereographic projection $\mathsf{R}^3 \to \mathsf{S}^3$) and collapse into localized structures [29]. Thus, there is an optimum $\rho_0$ value and, therefore, values of the characteristic momentum $\mathbf{c}$ and the $|L|/|Q|$ ratio at which the transition to a superconducting state results in the maximum energy gain. These problems are discussed in greater detail in Sections 4.3–4.6.

### 4.3 Rings versus stripes

We consider states outside the superconducting phase (the second line in the list of limit cases in Section 2.2). In this soft variant of the model, functional (2.3) takes the form

$$F = \int \mathrm{d}^3x \left[\frac{1}{4}\,\rho^2(\partial_k\mathbf{n})^2 + (\partial_k\rho)^2 + H_{ik}^2 - b\rho^2 + \frac{d}{2}\,\rho^4\right]. \quad (4.5)$$

In expression (4.5), the positive constant $\rho_0$ corresponds to the phase with a certain characteristic value of $b$.

It is well known from numerous experiments that in a phase state with the antiferromagnetic order destroyed by doping, the quasi-one-dimensional distributions of charge density $\rho_{\mathrm{h}}^2 = 1 - \rho^2$ have the form of stripes. The quasi-one-dimensional $\rho$-field configurations in (4.5) are actually favored because of the minimal free-energy loss due to the gradient term $(\partial_k\rho)^2$. Owing to the absence of gradient loss at the ends of closed configurations, the density distribution in the form of rings makes the smallest contribution to the energy compared with other quasi-one-dimensional configurations of density distribution.

We compare the contribution of quasi-one-dimensional distributions of $\rho^2$ in the form of rings and stripes to free energy (4.5) and compare the results of computations in [22] with experimental data. The following $\rho$ field configurations in the form of rings and stripes are chosen to serve as the trial functions:

$$\rho = \rho_0 \exp\left[-\frac{(r-r_0)^2}{2R_0^2}\right] \tag{4.6}$$

and

$$\rho = \rho_0 \exp\left(-\frac{x^2}{2L_x^2}\right) \begin{cases} 1\,, & |y| \leqslant L_y\,, \\ \exp\left[-\dfrac{\left(|y|-L_y\right)^2}{2L_x^2}\right], & |y| > L_y\,. \end{cases} \tag{4.7}$$

Here, $\rho_0 = \sqrt{b/d}$, $r_0$ is the radius and $R_0$ is the width of the ring, $2L_y = 2\pi r_0$ is the length of the stripe, and $L_x = R_0$ is its width. Configurations (4.6) and (4.7) being independent of the third coordinate, the size along it is assumed to be restricted by the length $L_z$, while $R_0 < r_0$ and $L_x < L_y$.

The computation of energy (2.5) with (2.6) and (2.7) taken into account gives the following result [22] for the contributions of the ring $F_r$ and the stripe $F_{xy}$ to the free energy:

$$F_r = \pi\rho_0^2 L_z \frac{\bar{r}_0}{R_0}\left(1+\frac{R_0^2}{\xi^2}\right), \tag{4.8}$$

$$F_{xy} = \pi\rho_0^2 L_z \frac{\bar{r}_0}{R_0}\left(1+\frac{R_0^2}{\xi^2}+\frac{R_0}{\bar{r}_0}+\left(n_0-\frac{3}{4}\,b\right)\frac{R_0^3}{\bar{r}_0}\right). \tag{4.9}$$

Here, $\bar{r}_0 = \sqrt{\pi}\,r_0$, $\xi^{-2} = 2\left[n_0 - (1-1/\sqrt{8})b\right]$, and $n_0$ is a certain characteristic value of the 'factor' $(\partial_k \mathbf{n})^2$ in (4.5) of the same order of magnitude as $c_1 R_0^{-2}$, while $b = c_2 R_0^{-2}\delta T$, where $c_i \sim 1$ and $\delta T = (T_c - T)/T_c$.

For the optimum width $R_0 = \xi$ (at $R_0 \ll r_0$), the difference between the free energies $\Delta F = F_{xy} - F_r$ in units $\pi\rho_0^2 L_z$ has the form

$$\Delta F = 1 + c_1 - c_2\,\delta T\,.$$

It follows from this expression that at $(1+c_1)/c_2 < 1$ in the temperature range

$$\left(1-\frac{1+c_1}{c_2}\right) < \frac{T}{T_c} < 1\,,$$

near the critical temperature $T_c$ of the transition to a state with a spin pseudo-gap, the preference should be given to ring configurations. In this state, the correlation length is $\xi \sim R_0 \sim 10$ Å. In the temperature range

$$T < T_c\left(1-\frac{1+c_1}{c_2}\right),$$

far from $T_c$, the leading configurations are given by stripes. It is known that $T_c$ can be approximated while maintaining a constant temperature by increasing the degree of doping. It is such experiments [55, 56] that have recently provided evidence of the existence of ring-shaped charge structures in underdoped phase states.

We consider the dependence of the critical temperature $T_c$ on the level of doping. For this, we represent the ratio of $F_r$ to $F_{xy}$ as

$$\frac{F_r}{F_{xy}} = \frac{1}{1+BR_0/\bar{r}_0}\,, \tag{4.10}$$

where

$$B = \frac{1}{2}\left[1+\frac{1}{2}\,\frac{n_0-3/4\,b}{n_0-(1-1/\sqrt{8})\,b}\right] = \frac{3}{4}\,\frac{n_0-0.68\,b}{n_0-0.65\,b}\,.$$

It follows that for $B < 0$, stripe configurations are energetically more favorable than ring-shaped configurations in the range $0.65 < n_0/b < 0.68$, where $F_{xy} < F_r$.

Normalization of the density $\rho_0^2$ to the number $N$ of doped particles with the condition $N = 2\pi r_0 \xi L_z m\rho_0^2$ yields the relation between $n_0$ and $b$ that can be written as $x = b/\sqrt{n_0 - 0.65b}$, where $x = Nd/(\sqrt{2}m\pi L_z r_0)$. For the boundaries of the above interval, when $n_0 \sim b \sim \delta T$, we obtain $T(p) = T_c(1 - A\,p^2)$ with the constant $A = (c_1 - 0.65\,c_2)/c_2^2$ and the level of doping $p = xR_0 = \sqrt{2}\,NR_0^2/(2\pi r_0 L_z)$. The factor $R_0^2/(2\pi r_0 L_z)$ in the last expression determines the degree of filling the three-dimensional space with quasi-one-dimensional configurations having the disturbed antiferromagnetic order.

In conclusion, we see that the 'level of doping – temperature' phase diagram inside the region corresponding to a phase state with the destroyed antiferromagnetic order contains a place for stripe-like charge structures. The relative contribution of rings and stripes to the free energy depends on the ratio of the correlation scale $R_0 \sim \xi$ to the characteristic length $r_0$ of filament configurations of the nonuniform exchange interaction field. The value of this parameter, whose geometrical meaning is discussed in Section 4.4, determines the gain in the free energy for closed (at $B > 0$) quasi-one-dimensional configurations.

### 4.4 Toroidal states

Closed quasi-one-dimensional configurations in the form of rings and stripes in model (2.3) with the free energy density

$$f = (\partial_k \rho)^2 + V_{\text{eff}}(\rho) + (F_{ik} - H_{ik})^2\,,$$

where

$$V_{\text{eff}} = -b_{\text{eff}}\,\rho^2 + \frac{d}{2}\,\rho^4$$

and

$$b_{\text{eff}} = b - \frac{1}{16}\,\mathbf{c}^2 - \frac{1}{4}\,(\partial_k \mathbf{n})^2\,,$$

exist in various phase states [57, 58]. In a phase where $b_{\text{eff}} < 0$, $\rho_{\min} = 0$. It follows from the expression for the effective potential energy $V_{\text{eff}}$ that nonuniform field distributions occur only in the case where $b_{\text{eff}} > 0$. As the degree of doping changes closer to the phase state with $b_{\text{eff}} > 0$, the relative number of quasi-one-dimensional configurations with closed ends increases. In the phase with $b_{\text{eff}} > 0$, quasi-one-dimensional configurations may have length $l$ satisfying the condition $l\rho_{\min} = 2\pi n$ [58].

In the ground state with the momentum $\mathbf{c} = 0$, the $\rho_{\min}$ value of the Higgs field amplitude is determined by the contribution $(1/4)(\partial_k \mathbf{n})^2$ from the characteristic $\mathbf{n}$-field configurations. In this case, the distributions in the form of

rings (as shown in Section 4.5) are the typical $\rho$-field configurations [22]. For larger values of the commensurability parameter $l\rho_{\min}$ ($l\rho_{\min} > 2\pi$) in the ground state, there are closed quasi-one-dimensional configurations of the field $\rho$. For the shorter ($0 < l\rho_{\min} < 2\pi$) $\rho$ field configurations, the ground state may exhibit quasi-one-dimensional field distributions in the form of stripes.

Thus, magnetically inhomogeneous phase states have the density-dependent internal hierarchical multiscale structure of critical importance for the description of the properties of these phases. Also, it is apparent that states with a finite value of the **c** momentum field are characterized by competing order parameters **n** and **c** between which nonlocal correlations arise due to the entanglement of their quasi-one-dimensional distributions.[1]

This inference is consistent with one of the main assertions in [60] that inhomogeneous current states cannot be described in a standard manner, in terms of the Ginzburg–Landau functional with a single vector order parameter. A similar conclusion is arrived at based on the lattice description of current states [9] in checker-ordered flow phases by considering the electron spin and charge degrees of freedom in model (2.4) in the mean-field approximation. Current phases [61–69] and the so-called d-density wave states [70–75], i.e., phases with current density modulations (and zero total current density), exemplify the realization of toroidal states [60, 61, 76].

The main feature of model (2.3) is the compactness of the **n** field accounting for its one-dimensional distributions in the form of knots and the discrete character of its spectrum (3.2). In this respect, the phenomenon in question is similar to the Berezinskii–Kosterlitz–Thouless effect, being its three-dimensional analog.

The present section focuses on the analysis of the general situation, with all nonuniform order parameters being present. We recall that in the case where $\mathbf{c} \neq 0$ and $\rho \neq \text{const}$, the characteristic size $R$ of a knot in the energy minimum $F_{\mathbf{n}}$ is proportional to $\rho^{-1}$. As the level of doping $\rho_{\text{h}}^2$ grows, i.e., as $\rho^2$ decreases, the radius $R \sim 1/\rho$ increases until it reaches the critical size $R_{\text{cr}} = \sqrt{2}$. It was shown in Section 4.1 that starting from this radius, knot-forming **n**-field configurations lose stability [29] with respect to perturbations associated with scale variations. This property is of primary importance in the comparison of different contributions to the free energy in inhomogeneous current states with a sufficiently small $\rho^2$ value.

To describe the distributions of strongly correlated charge and spin degrees of freedom at a sufficiently low density $\rho^2$, a small parameter $\alpha = R_0/R$ must be introduced, where $R_0$ is the correlation length of the **n** and **c** field distributions. Geometrically, the radius $R_0$ is the thickness of filaments on which field configurations are defined. The typical size of $R_0$ is of the order of 10 Å, i.e., equivalent to three or four lattice constants. The characteristic size of $R$ has the meaning [76] of the effective current correlation radius. In this case, the Ginzburg parameter is significantly smaller than unity, which justifies the use of the mean-field approximation in (2.3).

We suppose that $R_0 < R < R_{\text{cr}}$ and compare the decrease in free energy (2.3) due to the diamagnetic interaction $-2F_{ik}H_{ik}$ with its increase resulting from the nonuniform density distribution with $(\partial_k\rho)^2 \neq 0$. The contribution of the diamagnetic term $-2F_{ik}H_{ik}$ is of the order of $c_0/R_0^3$, where $c_0$ is the characteristic value of the field momentum **c**. The contribution of the term $(\partial_k\rho)^2$ is estimated as $1/(RR_0)^2$. Evidently, a gain in the energy due to $-2F_{ik}H_{ik}$ must also exceed the loss related to another positive term in (2.3), i.e., the surface term $F_{ik}^2 \sim c_0^2/R_0^2$ and the current energy density $\rho^2\mathbf{c}^2 \sim F_{ik}^2(R_0/R)^2$.

It follows from the combination of these inequalities that the momentum value at $\alpha = (R_0/R)^2 \ll 1$ satisfying the inequality

$$\frac{\alpha}{R_0} < c_0 < \frac{1}{R_0}\,, \tag{4.11}$$

the free energy, even in a state with the nonuniform distribution of the density $\rho^2$, may be smaller than at $\mathbf{c} = 0$ and $\rho = \text{const}$ due to the effective decrease in the contribution of the paramagnetic term $H_{ik}^2$.

The parameter $\alpha = R_0^2/R^2$ is proportional to the ratio of the volume occupied by a tangle of filaments to the ambient space. In other words, $\alpha$ has the meaning of the degree of filament packing in a three-dimensional tangle with a characteristic size $R$; it is actually the small parameter being sought in the situation of interest, where all coupling constants equal unity. This parameter enters the free energy ratio in (4.10) and the expression for the dependence of the temperature $T(p)$ on the degree of doping. For $\mathbf{n} = \text{const}$, the parameter $\alpha$ is proportional to $\kappa^{-2}$, where $\kappa = \lambda/\xi$ is the Ginzburg–Landau parameter and $\lambda$ is the London length.

Conditions for the existence of a state with an energy smaller than at $\mathbf{c} = 0$ and the momentum from interval (4.11) can be found by comparing the gain $c_0/R_0^3$ in the free energy density related to the term $-2F_{ik}H_{ik}$ and the contribution from the term $(\partial_k\rho)^2$. The loss of the total free energy is of the order of $R_z/R_0^2$, where $R_z$ is the vertical knot size. Thus, the condensation energy $-64\pi^2Q^{3/4}(L/Q)$ at $\rho = \text{const}$ and $L \ll Q$ decreases in the inhomogeneous case. The lowest gain $-\Delta F$ in the free energy for sufficiently flat knots with $R_0 < R_z < R < R_{\text{cr}}$ is estimated to be $\Delta F \simeq (64\pi^2/Q^{1/4})\alpha$. Thus, the energy of knotted configurations in inhomogeneous current states may be smaller than in the state with $\mathbf{c} = 0$.

For a sufficiently low doping level $\rho_{\text{h}}^2 = 1 - \rho^2 \ll 1$, the spin density $\rho^2$ is high and the knot size $R$ is so small that $\alpha \lesssim 1$. A decrease in the degree of filament packing in the knot with increasing $\rho_{\text{h}}$ is accompanied by a transition to a state in which field configurations in the form of closed quasi-one-dimensional distributions are favored over other planar projections $\rho(x, y)$ [22]. Whether the boundary charge states near the edges of dielectric islands form an infinite percolation cluster depends on the hole density $\rho_{\text{h}}^2$. This issue is discussed at greater length in Section 4.5.

We suppose that the level of doping is insufficient for the formation of an extended percolation cluster. This state with spontaneous superdiamagnetism is here called the toroidal state, as proposed by Ginzburg [76, 77]. A phase state in

[1] In a dynamic description in $(2+1)$-dimensional systems, nonlocal electron–electron interactions are described with the help of statistical Chern–Simons gauge fields $a_\alpha^i$ that give rise to strong long-range phase correlations between fermionic quantum states. In this case, the world-line linking matrix $k_{ij}$ in the Chern–Simons action

$$S = \frac{k_{ij}}{4\pi}\int_{\mathcal{M}} \mathrm{d}^3x\, \varepsilon_{\alpha\beta\gamma} a_\alpha^i \partial_\beta a_\gamma^j$$

is proportional [59] to the matrix $K_{\alpha\beta}$ in (3.7) describing the complexity of knotting and linking of one-dimensional field configurations in the $(3+0)$-dimensional free energy (2.3).

which the ordering of the diamagnetic surface current contours is characterized by a polar vector $T$ that changes sign upon time reversal may be associated with the ordering of local toroidal moments.

The toroidal moment is defined as [78 – 80]

$$\mathbf{a} = \operatorname{rot}\operatorname{rot}\mathbf{T}\,. \tag{4.12}$$

With this definition and the identity [18]

$$(\operatorname{rot}\mathbf{a})_i = \frac{1}{2}\,\varepsilon_{ikl}\,\mathbf{n}[\partial_k\mathbf{n}\times\partial_l\mathbf{n}]\,, \tag{4.13}$$

the toroidal moment can be expressed through the chiral density $\mathbf{n}\,[\partial_k\mathbf{n}\times\partial_l\mathbf{n}]$ as

$$T_i(\mathbf{r}) = \frac{1}{16\pi^2}\int \mathrm{d}^3r'\left[\frac{(\mathbf{r}-\mathbf{r}')_k}{|\mathbf{r}-\mathbf{r}'|^3}\int \mathrm{d}^3r''\,\frac{\mathbf{n}\,[\partial_k\mathbf{n}\times\partial_i\mathbf{n}]}{|\mathbf{r}'-\mathbf{r}''|}\right]. \tag{4.14}$$

The electrostatic and magnetostatic characteristics are combined in expression (4.14) in the form of a convolution of two multipliers. One of them has the form of the Bio – Savart law, and the other is defined by Coulomb Green's function. The vector **T** characterizes the distribution of the poloidal current component on the torus [79, 80]. The magnetic field of this current is localized inside the torus.

For the degree of spin distribution noncollinearity $\mathbf{n}\,[\partial_k\mathbf{n}\times\partial_i\mathbf{n}] = \varepsilon_{ki}\,\delta(\mathbf{r})$ localized at a point, the toroidal moment has the form

$$T_i(\mathbf{r}) = \frac{\varepsilon_{ki}}{16\pi^2}\int \mathrm{d}^3r'\,\frac{(\mathbf{r}-\mathbf{r}')_k}{r'|\mathbf{r}-\mathbf{r}'|^3} = \frac{\varepsilon_{ki}\,x_k}{8\pi r}\,. \tag{4.15}$$

If the chiral density

$$\mathbf{n}\,[\partial_k\mathbf{n}\times\partial_i\mathbf{n}] = \frac{\varepsilon_{ki}}{2\pi R}\,\delta(z)\,\delta(r-R)$$

of spin distributions is localized in the plane $z=0$ on a ring of radius $R$, the toroidal moment is $T_i(r, z=0) = \varepsilon_{ki}(x_i/r)t(r)$, where $t(r)$ is the function having a maximum at $r=R$, when $r \gg R$ $t(r)\sim r^{-2}$.

The diamagnetic susceptibility $\chi'$ in the toroidal state is determined [76] by the radius $R$ of electron current correlations such that $\chi' = \chi_{\mathrm{L}}/\alpha$, where $\chi_{\mathrm{L}} = -e^2k_{\mathrm{F}}/(12\pi^2mc^2)$ is the Landau diamagnetic susceptibility of noninteracting electrons. For porous knots with $\alpha \ll 1$, the diamagnetic susceptibility $\chi'$ is comparable to the ideal one, $\chi_{\mathrm{id}} = -1/4\pi$: $\chi' \sim -(10^{-3}-10^{-2})$, whereas for ordinary diamagnetic materials $|\chi'| \leqslant 10^{-4} \ll |\chi_{\mathrm{id}}|$. The abnormally high diamagnetic susceptibility is due to the large current correlation radius $R$. Also, it is worthwhile to note that the condition [81] $\chi_{\mathrm{L}} \sim -e^2nr^2/(mc^2) > -1/4\pi$, formally equivalent to the inequality $r < r_{\mathrm{D}} = c/\omega_{\mathrm{p}}$, reflects the boundary (surface) character of the phenomena under consideration. Here, $n$ is the mean electron density, $r_{\mathrm{D}}$ is the Debye radius, and $\omega_{\mathrm{p}} = (4\pi ne^2/m)^{1/2}$ is the plasma frequency.

The toroidal state is characterized by a zero total magnetic moment of a cluster, zero total magnetic field flux, and nonzero vector potential $\mathbf{A}(\mathbf{r}) = \big(3(\mathbf{nT})\mathbf{n}-\mathbf{T}\big)/r^3$. Similarly to a dipole field, the projection of the vector potential on the direction of **T** is proportional to the *d-symmetric* Legendre polynomial.

The place of the toroidal state in the classification of possible crystal states is determined by its symmetry properties. Of the total 122 magnetic classes, the toroidal state is inherent only in the systems belonging to 31 subclasses of magnetic symmetry in which the vector **T** can exist. Among these, there are, naturally, 10 classes containing no inversion of the direction of all the currents and therefore corresponding to the possibility of the pyroelectric effect.

The symmetry of media with a nonzero density of the toroidal moment allows the existence of the magnetoelectric effect [82]. In this case, the vector **T** is dual to the antisymmetric component of the magnetoelectric tensor. Media with the magnetoelectric effect may have no toroidal moment because media with $\mathbf{T} \neq 0$ give rise to a subset of the totality of 58 classes that may have the magnetoelectric effect. In the context of the representation theory of spatial magnetic groups, the toroidal state is structurally variable, comprising antitoroidal, noncollinear, disordered, and other structures.

Conditions for realization [81] of the toroidal state are easy to satisfy

- near inhomogeneities;
- in systems with strong electronic correlations;
- in an antiferromagnetic case where the toroidal phase being formed is the most probable state;
- under facilitating conditions in the presence of charged and magnetic impurities, such as holes and dynamically noncollinear spin distributions (in our case);
- in the case of strong spin – orbit interaction, which also promotes the manifestation of effects associated with toroidal ordering.

### 4.5 Planar phenomena in three-dimensional space

Under conditions where all coupling constants in expression (2.3) are equal to unity,[2] the main focus of study is the geometrical and topological properties of knotted one-dimensional manifolds in the domain of the order parameter definition making a leading contribution to the free energy. One result of such an approach is the appearance of a geometric parameter $\alpha = (R_0/R)^2 < 1$ that characterizes the degree of filament packing in the knot. The existence of a minimal field $\rho^2$ value playing the role of a current constant in expression (2.3), i.e., the minimal value of $\alpha_{\min} = (R_0/R_{\mathrm{cr}})^2$, is analogous to the existence of a nontrivial solution for the superconducting gap in a two-dimensional model [83] that emerges starting from a finite value of the coupling constant, unlike the solution in the framework of the BCS model.

The geometric properties of one-dimensional manifolds in the three-dimensional space are naturally considered [84, 85] in the context of the geometry of random planar images obtained at cross sections through a three-dimensional knot. Figure 2 gives an idea of the distribution [85, 86] of stratified phase states at one of the sections.

We choose the current parameter $\rho^2 \sim 1/R^2$ such that $\alpha_{\min} < \alpha \ll 1$ and project the spaces complementary to the knots and stretched over them (the so-called Seifert surfaces) onto the plane $xy$. In the theory of knots, Seifert surfaces provide an efficient tool for the search for algebraic knot characteristics. In the case under consideration, the Seifert surfaces are used to visualize distributions of the physical degrees of freedom.

For definiteness, we consider a trefoil knot, i.e., a knot with $Q=6$. Its complementary space is given by a triply twisted and glued ribbon and a Seifert surface in the form of a

[2] It is one of the reasons for the absence of even a numerical solution to the problem at hand.

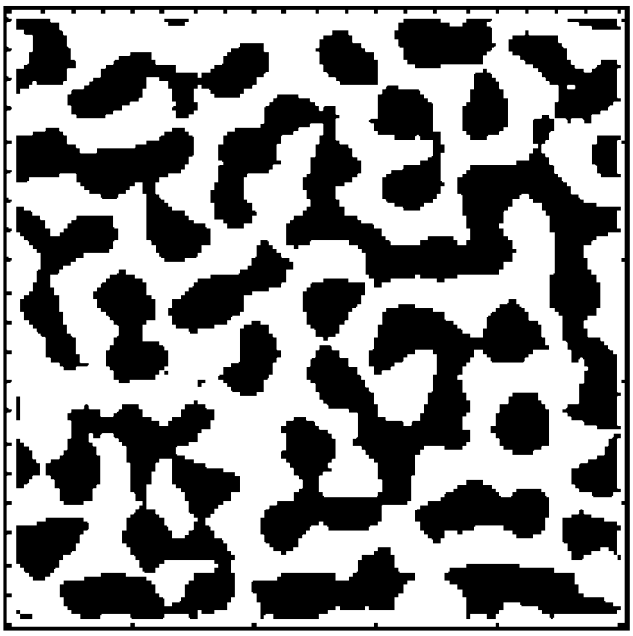

**Figure 2.** Two-dimensional distribution of phase states over the cross section through a tangle of knotted quasi-one-dimensional three-dimensional configurations of order parameters.

single-punctured torus (Fig. 3).[3] As mentioned above, the charge degrees of freedom are distributed starting from the edge of the complementary space for the knots. Let the area of the part of the region related to the Seifert surface projection on the plane be small compared with the knot projection area. For an essentially flat knot [87] with $R_z < R < R_{cr}$, the boundary region is a ring formed by the projection of these one-dimensional edge configurations onto the plane. For a knot elongated at $R < R_z < R_{cr}$ along the $z$ axis, the edge line is equivalent to a stripe of length $R$, equal to the scale of the hole at the torus projected on the plane. As a result, the gain in free energy in an inhomogeneous toroidal state is achieved if the charge density is distributed over the plane in the form of rings.

Investigations into such charge density configurations are carried out with the use of tunneling microscopy. Formation of ring-shaped state density distributions was recently discovered in experiments [56] on complicated labyrinth structures of quasi-one-dimensional charge density distributions in planar compounds $Ca_{2-x}Na_xCuO_2Cl_2$ at a moderate doping level $x$.

### 4.6 Optimal doping

At a sufficiently low doping level, the knot size $R$ is so small that $\alpha \lesssim 1$. A decrease in the degree of filament packing in the knot, $\alpha$, with increasing $\rho_h$ results in the transition to a state in which field configurations in the form of closed quasi-one-dimensional distributions are favored over other planar projections $\rho(x, y)$ [22]. Whether the phase state at $\alpha_{cr} < \alpha \ll 1$ and the finite momentum of electron pairs $\mathbf{c}_0$ [50, 51] is superconducting or proves to be an intermediate state with spontaneous diamagnetism [76, 81] probably depends on the degree of linking of a totality of planar current clusters (see, e.g., Ref. [88]) formed by projections of the Seifert surfaces onto the plane.

It is natural to assume [89] that the appearance of the preliminarily formed pairs in an underdoped state and phase coherence in a superconducting phase are independent phenomena. Starting from the picture of previously formed pairs, we consider certain peculiarities of phase coherence conditioned by percolation phenomena [90], bearing the aforementioned charge density structures in mind. As the hole density $\rho_h^2$ increases, the size of ring-shaped current distributions becomes so large that a two-dimensional coherent current cluster may appear and the transition to a state with momentum $\mathbf{c} \neq 0$ occurs, with a gain in the free energy. We find the doping level $p_{best}$ at which the temperature of transition to the superconducting state is maximum.

If we did not take distributions of the charge degrees of freedom at the boundaries of **n**-field filamentous configurations in the knot into account, we would have to deal with the two-dimensional percolation problem and the generally known [88] result $p_{cr} = 0.5$ for the critical density value in the bond percolation problem. An essential difference between the experimentally found value $p_{best,\,exp} = 0.16$ and the above critical value provides a convenient test for the verification of the validity of the approach being considered.

We use the recently obtained experimental data [56] for the purpose of this verification. It was demonstrated in [56] with the use of scanning tunneling microscopy that a fraction of filamentous field distributions in the form of ring-shaped structures in a milieu of quasi-one-dimensional configurations with an increasing charge state density in the underdoped region grows with the level of doping.

Using trial functions, we arrived at the conclusion that in the framework of model (2.3), such configurations are actually favored when the level of doping is increased. The distribution patterns of the spin degrees of freedom in underdoped states are evaluated and interpreted based on neutron scattering data and on the assumption of quasi-one-dimensional nanoscale distributions in the planes of charge clusters in the form of thin rings.

Let the edge points lie along the boundaries of ring-shaped dielectric regions such that the ring width differs from the diameter (as follows from the experiment in Ref. [56]) by approximately $\alpha^{1/2} = R_0/R \simeq 0.1$. The geometric confinement allows the contribution of internal (relative to ring-shaped charge configurations) spin distributions of the degrees of freedom to be attributed to the normalization background. Therefore, for the threshold of the emergence of a connected cluster formed by the ideal distribution in the form of rings, the value $p_{best} = 0.5 - \pi\alpha^{1/2} = 0.186$ is significantly smaller than the standard $p_{cr} = 0.5$. For a hexahedral current cell, $p_{best} = 0.179$. This example indicates that even relatively small deviations in the shape of an elementary current cell from the ideal ring-shaped form may result in the convergence of the $p_{best}$ value and the experimentally found $p_{best,\,exp} = 0.16$. Consideration of a square bounded by stripe-like charge distributions instead of a circular dielectric cluster yields $p_{best} = 0.5 - 4\alpha^{1/2} = 0.1$.

Investigations into the general properties of phase states in high-temperature superconductors representing different classes of chemical compounds, e.g., $Y_{1-x}Ca_xBa_2Cu_3O_6$ or $La_{2-x}Sr_xCu_4$, have demonstrated that the dependence of the critical temperature on the hole concentration is fairly well approximated [91, 92] by the curve $T_c/T_{c,\,max} =$

[3] A thread entangled into a trefoil extended along the time axis can be regarded in a dynamic $(2+1)$-dimensional case as a result of the action of $b_1^3$ on quantum states of the braid group operator $b_1$.

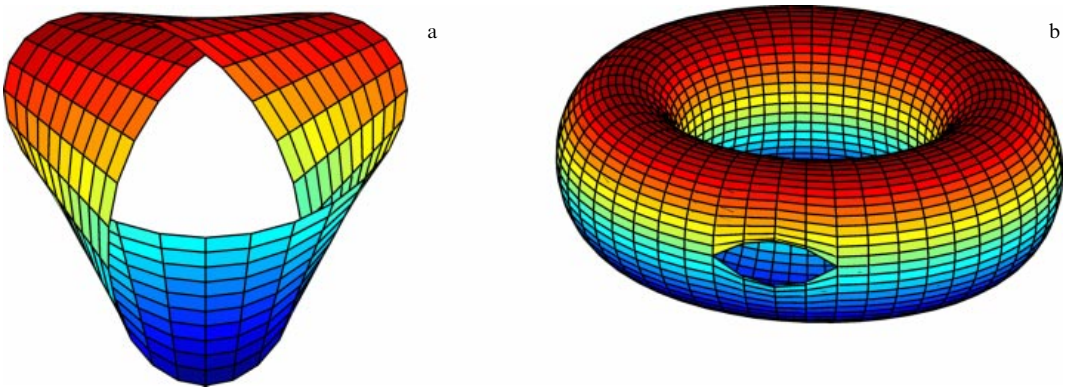


**Figure 3.** Surfaces spread out over a flat trefoil (a) and a trefoil elongated along the $z$ axis (b).

$1 - 82.6(p - 0.16)^2$ at $p = x/2$. The parabolic dependence $T_c(p)$ has zeroes at $p_{\min} \approx 0.05$, $p_{\max} \approx 0.27$ and reaches a maximum at $p_{\text{best}} = 0.16$. In optimally doped thallium-based compounds, e.g., in $Tl_{0.5}Pb_{0.5}Sr_2Ca_{0.8}Y_{0.2}Cu_2O_7$, $p_{\text{best}} = 0.15$. Similar values have been obtained in studies with some other classes of high-temperature superconductors. It is also noteworthy that an underdoped pseudogap phase with large charge and spin fluctuations arises in the background of the superconducting state in the aforesaid classes of chemical compounds with a well-defined [93] hole concentration, $p \approx 0.19$.

## 5. Non-Abelian gauge theory

### 5.1 Monopoles, merons, and knots in the Yang – Mills theory

Thus far, we have considered the nonrelativistic $(3+0)$-dimensional model with the solution of equations of motion in the form of quasi-one-dimensional knotted field configurations. The relativistic theory of knots [1, 94] is the Yang – Mills gauge theory. A variety of methods for mixing Lorentz indices and indices of the internal degrees of freedom of the potentials in the non-Abelian gauge theory provides a possibility to universally describe [94] point-like monopole configurations and extended objects in the form of knots. In the ultraviolet region, the theory is described by the standard Yang – Mills action

$$S = \frac{1}{g^2}\int \mathrm{d}^4x \ \mathrm{Tr}\,\mathbf{F}_{\mu\nu}^2\,, \tag{5.1}$$

where

$$\mathbf{F}_{\mu\nu} = \partial_\mu \mathbf{A}_\nu - \partial_\nu \mathbf{A}_\mu + [\mathbf{A}_\mu, \mathbf{A}_\nu]\,, \tag{5.2}$$

and $g$ is the bare coupling constant.

The most *complete* ansatz [94 – 96] for parameterization of SU(2) potentials $\mathbf{A}_\mu = A_\mu^a \tau^a/2\mathrm{i}$, where $\tau^a$ are the Pauli matrices, has the form

$$A_\mu^a = C_\mu n^a + \sigma\,\partial_\mu n^a + (1+K)\varepsilon_{abc} n^c\,\partial_\mu n^b\,. \tag{5.3}$$

Gauge-fixed four-dimensional SU(2) connections $\mathbf{A}_\mu$ contain six degrees of freedom [94], viz. two transverse polarizations of the U(1) potentials $C_\mu$, two independent components of the unit vector field $n^a$, and two scalar functions $\sigma$ and $K$. The scalars $\sigma$ and $K$ are convenient to combine into a complex field $\phi = \sigma + \mathrm{i}K$ entering a multiplet $(C_\mu, \phi)$ that transforms as the multiplet in the Abelian Higgs model. One property of the $(C_\mu, \phi)$ multiplet is that the functional form of $A_\mu^a$ is preserved under SU(2) gauge transformations with the parameter $\alpha^a = \alpha n^a$.

The computation of the tension

$$\mathbf{F}_{\mu\nu} = \mathbf{n}\big\{G_{\mu\nu} - \big[1 - (\sigma^2 + K^2)\big]H_{\mu\nu}\big\} + (D_\mu\sigma\,\partial_\nu\mathbf{n} - D_\nu\sigma\,\partial_\mu\mathbf{n}) + \big(D_\mu K[\partial_\nu\mathbf{n}\times\mathbf{n}] - D_\nu K[\partial_\mu\mathbf{n}\times\mathbf{n}]\big)\,, \tag{5.4}$$

and variation of action (5.1) with respect to the fields $C_\mu$, $\phi$, and $\mathbf{n}$ lead to the equations of motion

$$\mathbf{n}\,\nabla_\mu\mathbf{F}_{\mu\nu} = 0\,, \tag{5.5}$$

$$\partial_\nu\mathbf{n}\,\nabla_\mu\mathbf{F}_{\mu\nu} = 0\,, \tag{5.6}$$

$$[\partial_\nu\mathbf{n}\times\mathbf{n}]\,\nabla_\mu\mathbf{F}_{\mu\nu} = 0\,, \tag{5.7}$$

$$(D_\nu\sigma + D_\nu K\mathbf{n})\,\nabla_\mu\mathbf{F}_{\mu\nu} = 0 \tag{5.8}$$

that are proportional to the Yang – Mills equations $\nabla_\mu\mathbf{F}_{\mu\nu} = 0$ derived using potentials (5.3). Here, $D_\mu = \partial_\mu + \mathrm{i}C_\mu$ and $\nabla_\mu$ are the U(1)- and SU(2)-covariant derivatives, respectively, $G_{\mu\nu} = \partial_\nu C_\mu - \partial_\mu C_\nu$, and $H_{\mu\nu} = \mathbf{n}\,[\partial_\mu\mathbf{n}\times\partial_\nu\mathbf{n}]$.

That the density of the Lagrangian function $L$ contains a structure responsible for the appearance of the term $F_{\mathbf{n}}$ in expression (2.3) can be seen in the case where $C_\mu = \sigma = 0$. Then,

$$L = \frac{2}{g^2}\big\{\delta_{\mu\nu}(\partial_\lambda\mathbf{n})^2 - (\partial_\mu\mathbf{n})(\partial_\nu\mathbf{n})\big\}\,\partial^\mu K\partial^\nu K - \frac{1}{g^2}\big\{\mathbf{n}\,[\partial_\mu\mathbf{n},\partial_\nu\mathbf{n}]\big\}^2(K^2-1)^2\,. \tag{5.9}$$

It follows from expression (5.9) that due to factorization of the kinetic and potential items, the braced multipliers in front of the right-hand terms corresponding to the kinetic and potential energies play the role of current coupling constants for the field $K$ and vice versa. Therefore, it is possible to obtain the first two terms in (2.3) after averaging over $K$, under the condition that $\mathbf{n} \neq \mathbf{r}/r$.

The requirement that the vector $\mathbf{n} = \mathbf{r}/r$ at each point with coordinates given by the radius vector $\mathbf{r}$ be directed toward this point essentially fixes the $\mathbf{n}$-field dynamics. In this case, the problem is substantially simplified. Indeed, in such a

'hedgehog' variant, $A_k^a = \varepsilon^{akc} n^c (K+1)/r$ and

$$\left\{\delta_{\mu\nu}(\partial_\lambda \mathbf{n})^2 - (\partial_\mu \mathbf{n})(\partial_\nu \mathbf{n})\right\} = \frac{\delta_{\mu\nu}}{r^2}\,, \qquad \left(\mathbf{n}\,[\partial_\mu \mathbf{n}, \partial_\nu \mathbf{n}]\right)^2 = \frac{1}{r^4}\,.$$

The density of the Lagrange function and the equation of motion for the scalar field $K(r,t)$ take the form

$$L = \frac{2}{g^2 r^2}(\partial_\mu K)^2 - \frac{1}{g^2 r^4}(K^2-1)^2\,, \tag{5.10}$$

$$r^2 \Box K = K(K^2-1)\,, \qquad \Box = \frac{\partial^2}{\partial t^2} - \frac{\partial^2}{\partial r^2}\,. \tag{5.11}$$

The singular solution of the equations of motion, $K = 0$, leads to the Wu–Yang monopole configuration $A_k^a = \varepsilon^{akc} n^c / r$ [97]. In this case, smooth **n**-field distributions used in the expression for the potential, $A_i^a = \varepsilon_{abc}\partial_i n^b n^c$, describe monopole condensation.

The simplest solution of Eqns (5.11) is the meron configuration, $K = t/\sqrt{t^2 - r^2}$ [98]. A meron, being a solution of the equations of motion, is characterized by the topological charge 1/2 and a logarithmically divergent action. Multimeron $K$-field distributions have been considered in Refs [98–101] with the use of the cylindrically symmetric ansatz [102, 103] contained in expression (5.3) with $\mathbf{n} = \mathbf{r}/r$. A common property of the solutions of Eqn (5.11) is the presence of $K$-field singularities at closed surfaces located at a finite distance from the origin $\mathbf{r} = 0$ [101]. Such singularities allow considering the infrared limit in a situation where the **n**-field color degrees of freedom are collinear to the radius vector **r**.

The opposite limit case corresponds to the consideration of the **n**-field orientational dynamics while fixing the $K$ field scalar degrees of freedom. In this case, the possible phase states [57, 58, 104, 105] in the Yang–Mills theory can be studied by means of functional integration over the Abelian Higgs multiplet and subsequent gradient expansion of the Wilson effective action for the order parameter **n**. This problem was scrutinized in Refs [106–109], where it was shown that the total effective action for low-energy degrees of freedom of **n** in the Yang–Mills theory must contain the two terms known from (2.3) in the combination

$$L = \frac{\mu^2}{2}(\partial_\mu \mathbf{n})^2 - \frac{\alpha}{4}\left(\mathbf{n}\,[\partial_\mu \mathbf{n}\,\partial_\nu \mathbf{n}]\right)^2\,, \tag{5.12}$$

where $\mu$ is the mass scale and $\alpha$ is the effective coupling constant. Expression (5.12) contains not only the first mass term determining the long-range dynamics of the **n** field and absent in the massless theory (5.1) but also additional terms with derivatives of the form $(\partial_\mu \mathbf{n})^4$ and $(\partial^2 \mathbf{n}\,\partial^2 \mathbf{n})$ (provided the lowest loop diagrams are taken into account) [106–109]. Because

$$(\mathbf{n}\,\partial_\mu \mathbf{n} \times \partial_\nu \mathbf{n})^2 = (\partial \mathbf{n})^4 + (\partial_\mu \mathbf{n}\,\partial_\nu \mathbf{n})^2\,,$$

there is no reason to expect that both terms in this expression must have equal coupling constants after the renormalization.

The hypothesis in [94] of the infrared limit in the Yang–Mills theory in form (5.12) was motivated by the necessity to obtain the desired Hamiltonian action structure, which implies the absence of the third and higher time derivatives. It was shown in Refs [106–109] that the covariant renormalization-group approach disregards the Hamiltonian interpretation of the final result — the sought simplification is corrupted by the emergence of the terms with the derivatives of the form $(\partial_\mu \mathbf{n})^4$ and $(\partial^2 \mathbf{n}\,\partial^2 \mathbf{n})$. We note that the general conclusion concerning the existence of knotted soliton-like **n**-field configurations as important infrared degrees of freedom in the Yang–Mills theory remains valid.

The simplest analysis of the case where $\mathbf{n} \neq \mathbf{r}/r$ with the unknown function $K$ can be performed by substituting the last term in (5.3) into the self-duality equations. For the low symmetry under consideration [28],

$$G = \mathrm{diag}\left[\mathrm{O}(2)_\mathrm{I} \otimes \mathrm{O}(2)_\mathrm{S}\right]\,,$$

where $\mathrm{O}(2)_\mathrm{I}$ and $\mathrm{O}(2)_\mathrm{S}$ are the groups of rotations about the respective axes $N_3$ and $z$, these equations (differing from the equations in the spherically symmetric [110, 111] and axially symmetric [102, 103] cases) have the form [112]

$$[\partial_\tau \mathbf{n}, \partial_k \mathbf{n}] = \frac{1}{2}\,\varepsilon_{kms}\,[\partial_m \mathbf{n}, \partial_s \mathbf{n}]\,, \tag{5.13}$$

$$\partial_\tau K \partial_k \mathbf{n} - \partial_k K \partial_\tau \mathbf{n} = \frac{1}{2}\,\varepsilon_{kms}\left\{\partial_m K \partial_s \mathbf{n} - \partial_s K \partial_m \mathbf{n}\right\}\,, \tag{5.14}$$

where $\tau = \mathrm{i}t$ is the Euclidean time. Because the homotopy group $\pi_4\big(\mathrm{SU}(2)\big) = \mathsf{Z}_2$ is nontrivial [113], there is at least one nontrivial class of the $K$ and **n** field configurations.

### 5.2 Knots as ground states

It was proposed in Refs [59, 114] to interpret SU(2) vacuum configurations of gauge fields in terms of knots. We consider such an approach based on the use of the Abelian projection.

The idea of the Abelian projection was put forward in Refs [104, 105] in order to decompose a non-Abelian field into its neutral and charged components under an appropriate gauge choice. In the simplest form, the Abelian projection involves the choice of a certain observable $X(x)$, such as Polyakov's exponential, undergoing gauge transformations $g^\dagger(x)\,X(x)\,g(x)$. This fact may be used for the diagonalization of $X(x)$, which can be performed smoothly if the matrix $g$ has no coincident eigenvalues. The remaining gauge freedom is $\mathrm{U}(1)^r$, where $r$ is the rank of the gauge group. The degrees of freedom in such a gauge are associated with $r$ via neutral bosons.

Singularities appear when two or more eigenvalues coincide. The coincidence leads to point-like singularities that represent magnetic monopoles defined with respect to the residual Abelian gauge group. A smoother but nonlocal Abelian gauge fixing can be introduced [104] using the Abelian field as a background [e.g., the SU(2)-component proportional to $\tau_3 = \mathrm{diag}\,(1,-1)$] and imposing the background gauge condition on the charged component $A_\mu^{\mathrm{ch}}$ of the gauge field. The gauge condition can be formulated by minimizing the functional integral $\int |A_\mu^{\mathrm{ch}}|^2$ over the gauge orbits.

The Abelian projection allows identifying the field $\mathbf{n}(x)$ of the nonlinear O(3) sigma-model with the local color direction in the SU(2) gauge theory. General doubts about the validity of such an approach arise from the fact that gauge invariance precludes independent dynamics of magnetic variables associated with the color direction. An analysis of the possibilities points out the necessity of introducing the dual variables considered in Section 5.5. Moreover, the Goldstone bosons [114] associated with the spontaneous O(3)-symmetry violation in the nonlinear sigma-model in the dimension

$(3+1)$ are undesirable in the particle-free non-Abelian gauge theory.

Following [59, 115], we now show that the field $\mathbf{n}$ expressed via $CP^1$-variables can be related to the SU(2) gauge field of zero strength. This leads to the interpretation of such pure-vacuum configurations (in a particular maximum Abelian gauge) in terms of knots with the Hopf invariant given by the winding number of gauge configurations. In this identification, $\left(\partial_\mu \mathbf{n}(x)\right)^2 = 4|A_\mu^{\mathrm{ch}}|^2$. We consider the effective low-energy representation of the SU(2) gauge theory with the $(3+1)$-dimensional action defined in terms of the unit vector field $\mathbf{n}(x)$ as

$$S = \int \mathrm{d}^4x \left( \partial_\mu \mathbf{n}(x)\, \partial^\mu \mathbf{n}(x) - \frac{1}{2} F_{\mu\nu} F^{\mu\nu} \right) \tag{5.15}$$

with the gauge field strength

$$F_{\mu\nu} = \frac{1}{2}\, \mathbf{n}(x) \left( \partial_\mu \mathbf{n}(x) \wedge \partial_\nu \mathbf{n}(x) \right).$$

Using the possibility of rescaling the action and coordinates, we assumed in (5.12) that $\mu^2 = \alpha = 2$ and used compact notation of differential geometry. The variables $\partial_\mu \mathbf{n}(x)$ of the three-dimensional unit vector being orthogonal to $\mathbf{n}(x)$, $\partial_\mu \mathbf{n}(x) \wedge \partial_\nu \mathbf{n}(x)$ is proportional to $\mathbf{n}(x)$ with the proportionality factor $2F_{\mu\nu}(x)$. Hence,

$$F_{\mu\nu}^2 = \frac{1}{4} \left( \partial_\mu \mathbf{n}(x) \wedge \partial_\nu \mathbf{n}(x) \right)^2 .$$

The finite energy value

$$E = \int \mathrm{d}^3x \left[ \left( \partial_i \mathbf{n}(x) \right)^2 + \frac{1}{2} F_{ij}^2(x) \right] \geqslant c|Q|^{3/4} \tag{5.16}$$

requires that $\mathbf{n}(\mathbf{x})$ tend to a constant vector at spatial infinity. The value of the constant $c = 16\pi^2 3^{3/8} \sim 238$ was corrected in Ref. [29].

The two degrees of freedom associated with the field $\mathbf{n}$ are equivalent to the two components of the $CP^1$-field $\Psi$ defined up to a common scaling complex unimodular factor. This follows from the relation

$$n^a(x) = \Psi^\dagger(x) \tau^a \Psi(x) . \tag{5.17}$$

The Abelian gauge invariance of the $CP^1$ model leads to the composite gauge field

$$A_\mu(x) = -\mathrm{i} \Psi^\dagger(x)\, \partial_\mu \Psi(x) . \tag{5.18}$$

Direct computation may be used to verify that the 2-form $F(x) = \mathbf{n}(\mathbf{x}) \left( \mathrm{d}\mathbf{n}(\mathbf{x}) \wedge \mathrm{d}\mathbf{n}(\mathbf{x}) \right)$ exactly defines the 1-form $A(x)$ of the Abelian gauge field by the relation $F(x) = \mathrm{d}A(x)$. In terms of the potential $A(x)$, the density of the Hopf invariant is given by $A(x) \wedge F(x)$. The following useful relations are used in the computation: $\delta_{ij}\delta_{kl} + \tau_{ij}^a \tau_{kl}^a = 2\delta_{il}\delta_{jk}$ and $\mathrm{i}\varepsilon_{abc} \tau_{ij}^b \tau_{kl}^c = \tau_{kj}^a \delta_{il} - \tau_{il}^a \delta_{jk}$.

In this formulation,

$$S = \int \mathrm{d}^4x \left( 4 (D_\mu \Psi)^\dagger(x)\, D^\mu \Psi(x) - \frac{1}{2} F_{\mu\nu}(x) F^{\mu\nu}(x) \right), \tag{5.19}$$

where $D_\mu = \partial_\mu - \mathrm{i}A_\mu(x)$ is the covariant variable, $\Psi^\dagger(x) D_\mu \Psi(x) = 0$, and $E = \int \mathrm{d}^3x \left| \left( 2D_i + B_i(\mathbf{x}) \right) \Psi(\mathbf{x}) \right|^2$ with $B_i = 1/2\varepsilon_{ijk} F_{jk}$.

At the next step of model reformulation, it is assumed that any two-component complex vector with unit length uniquely corresponds to an element $g(x)$ of the SU(2) group. Therefore, it is possible to write $\Psi(x) = g(x)\Psi_0$. For convenience, we choose $\Psi_0^\dagger = (1, 0)$, such that

$$n^a(x) = \frac{1}{2}\, \mathrm{Tr} \left( \tau_3 g^\dagger(x)\, \tau_a g(x) \right). \tag{5.20}$$

We introduce the currents $J_\mu(x) \equiv \mathrm{i}\tau_a J_\mu^a(x) \equiv g^\dagger(x)\, \partial_\mu g(x)$. They can be interpreted as components of the gauge SU(2)-connection with zero tension, i.e., $G(x) = \mathrm{d}J(x) + J(x) \wedge J(x) = 0$, where $J(x) \equiv J_\mu(x)\, \mathrm{d}x_\mu$. Writing in the components gives

$$G_{\mu\nu}^a(x) = \partial_\mu J_\nu^3(x) - \partial_\nu J_\mu^3(x) - 2\left( J_\mu^1(x) J_\nu^2(x) - J_\nu^1(x) J_\mu^2(x) \right) = 0 .$$

Simple calculation yields

$$A_\mu(x) = J_\mu^3(x) , \qquad \partial \Psi_\mu^\dagger(x)\, \partial^\mu \Psi(x) = J_\mu^a(x)\, J_a^\mu(x) . \tag{5.21}$$

The zero tension of the non-Abelian field accounts for the identity

$$F_{\mu\nu}(x) = 2\left( J_\mu^1(x) J_\nu^2(x) - J_\nu^1(x) J_\mu^2(x) \right), \tag{5.22}$$

or

$$F(x) = \mathrm{d}J^3(x) = 2J^1(x) \wedge J^2(x) \tag{5.23}$$

in terms of $J^a \equiv J_\mu^a(x)\, \mathrm{d}x_\mu$.

Now, it is easy to show [59, 115, 116], with the help of relation (5.22) and using $J(x) = g^\dagger(x)\, \mathrm{d}g(x)$, that the Hopf invariant is exactly equal to the winding number of the gauge function $g(\mathbf{x})$:

$$\frac{1}{4\pi^2}\, A(\mathbf{x}) \wedge F(\mathbf{x}) = \frac{1}{2\pi^2}\, J^3(\mathbf{x}) \wedge J^1(\mathbf{x}) \wedge J^2(\mathbf{x}) = \frac{1}{24\pi^2}\, \mathrm{Tr} \left( g^\dagger(\mathbf{x})\, \mathrm{d}g(\mathbf{x}) \right)^3 . \tag{5.24}$$

We recall that the gauge function $g(\mathbf{x})$ enters the relation $n^a(\mathbf{x})\tau^a = g(\mathbf{x})\tau_3\, g^\dagger(\mathbf{x})$ and defines the SU(2) gauge potential $J(\mathbf{x})$ with zero tension. Certainly, it is possible to express [106] the left-hand side of (5.24) via the density of the non-Abelian Chern – Simons term:

$$\frac{1}{4\pi^2}\, A(\mathbf{x}) \wedge F(\mathbf{x}) = -\frac{1}{8\pi^2}\, \mathrm{Tr} \left( J(\mathbf{x}) \wedge \mathrm{d}J(\mathbf{x}) + \frac{2}{3}\, J(\mathbf{x}) \wedge J(\mathbf{x}) \wedge J(\mathbf{x}) \right). \tag{5.25}$$

To see that static solutions of the model in (5.15) are actually ground states of the classical Yang – Mills model in the nonlinear maximally Abelian gauge, we consider the relation

$$(D_\mu \Psi)^\dagger(x)\, D^\mu \Psi(x) = \partial_\mu \Psi^\dagger(x)\, \partial^\mu \Psi(x) - A_\mu(x) A^\mu(x) = J_\mu^1(x)\, J_1^\mu(x) + J_\mu^2(x)\, J_2^\mu(x) . \tag{5.26}$$

In the absence of the neutral component $J_\mu^3(x)$, relation (5.26) reflects the nature of the action of model (5.19) in

$SU(2)/U(1)$, because both terms in (5.19) are expressed only through $J_\mu^1(x)$ and $J_\mu^2(x)$. Specifically, the static configuration energy is expressed only through the charged components of the non-Abelian gauge field:

$$E = \int \mathrm{d}^3x \left(4\left(J_i^1(\mathbf{x})\, J_i^1(\mathbf{x}) + J_i^2(\mathbf{x})\, J_i^2(\mathbf{x})\right) + 2\left(J_i^1(\mathbf{x})\, J_j^2(\mathbf{x}) - J_j^1(\mathbf{x})\, J_i^2(\mathbf{x})\right)^2\right). \tag{5.27}$$

Here, the first term exactly corresponds to the functional determining the maximally Abelian gauge by means of minimization along the gauge orbits that leave the $\tau_3$-generated Abelian subgroup fixed [104]. This assertion also holds for the total functional (5.27) because it can also be interpreted as a gauge-fixing functional in the case of the nonlinear maximally Abelian gauge. As long as the three parameterizations are equivalent, there is every reason to interpret functional minima for the energy in the sector with a given $Q$ value as gauge-fixed pure-gauge connections (i.e., zero-tension potentials) in the sector with the gauge field winding number $Q$.

Difficulties in interpreting model (5.15) as an effective low-energy representation of the SU(2) gauge theory [94, 106, 117] mentioned in this section and in Section 5.1 seem to occur because the perturbative expansion near the state $\mathbf{A}_\mu(x) = \partial_\mu \mathbf{n}(x) \wedge \mathbf{n}(x)$ [at $C_\mu = \sigma = K = 0$ in (5.3)] is invalid because this state corresponds to a local energy maximum and is unstable [59].

This inference is supported by the consideration of a one-parameter family of potentials in the form $\mathbf{A}_\mu(x) = q\,\partial_\mu \mathbf{n}(x) \wedge \mathbf{n}(x)$ with a certain constant $q$. The estimated field strength

$$\mathbf{F}_{\mu\nu}(\mathbf{x}) = q(q-2)\,\partial_\mu \mathbf{n}(\mathbf{x}) \wedge \partial_\nu \mathbf{n}(\mathbf{x}) \tag{5.28}$$

is nonzero at $q = 1$. The energy of this state, proportional to $q^2(q-2)^2$, actually has a maximum at $q = 1$. This accounts for its instability.

On the other hand, the background energy vanishes not only in the case of the trivial vacuum at $q = 0$ but also at $q = 2$. The latter case corresponds to the pure-gauge potential $J$ having a topological charge $Q$ that is defined by the integral over the density space of the non-Abelian Chern–Simons term. Multiplication of the pure-gauge connections of $J$ by $q/2$ readily yields the integral of the non-Abelian Chern–Simons density at any $q$. This integral equals $q^2(3-q)Q/4$. The relation between the Hopf invariant and the non-Abelian Chern–Simons term at $q = 1$ was also found in Ref. [106]. It should be noted that the integral gives half the Hopf invariant at $q = 1$. Therefore, this background distribution of the gauge potential lies in a sense halfway between two vacua.

The pure-gauge background with $q = 2$ is useful in solving the problem of categorizing gauge fields by their different topological sectors because small fluctuations parameterized with the help of the functions $C_\mu$, $\sigma$, and $K$ do not change the winding number. Under these conditions, which could be called the Faddeev–Niemi gauge-fixing conditions, the categorization by different topological sectors is possible in the localized form irrespective of the gauge field asymptotic behavior. This observation may bring about a new understanding of the approach to the nontrivial topology of non-Abelian gauge theories.

To conclude, there is a gauge at which gauge vacua with different winding numbers $Q$ can be characterized using nonequivalent knots. Topological [118] and conformal [119] field theories allow finding the relation between the invariants for torus knots $\mathcal{T}(s,t)$ with $Q = st$ and the properties of minimal models $\mathcal{M}(s,t)$ with the central charge $c(s,t) = 1 - 6(s-t)^2/(st)$ in the case of coprime integers $s$ and $t$. The relation to monopoles and instantons [106, 120] that interpolate between knots of different types and connect vacua are discussed in Sections 5.3–5.6.

### 5.3 Skyrmions and knots

The construction establishing the interconnection between instantons and knots [29] relates the instantons to solutions of the Skyrme problem [121, 122]. For this reason, a consistent detailed description should be preceded by a discussion of the main properties of skyrmions and their relation to instantons [123]. Following [124], it is convenient to begin from the formulation of the Skyrme model [121, 122] and thereafter move to the discussion of a one-parameter family of models that includes the Skyrme and Skyrme–Faddeev models.

Using the standard units of length and energy, the Skyrme Lagrangian can be written as

$$L = \int \mathrm{d}^3x \left\{-\frac{1}{2}\,\mathrm{Tr}\,(R_\mu R^\mu) + \frac{1}{16}\,\mathrm{Tr}\,\left([R_\mu, R_\nu][R^\mu, R^\nu]\right)\right\}. \tag{5.29}$$

This expression involves the current $R_\mu = (\partial_\mu U)U^+$ depending on an arbitrary matrix $U$ taking values in the SU(2) group. The equations of motion ensuing from Eqn (5.29) are nonlinear equations for the matrix $U(t,\mathbf{r})$ and have the form of the current conservation law $\tilde{R}^\mu = R^\mu + (1/4)\left[R^\nu, [R_\nu, R^\mu]\right]$:

$$\partial_\mu\left(R^\mu + \frac{1}{4}\left[R^\nu, [R_\nu, R^\mu]\right]\right) = 0\,. \tag{5.30}$$

With the boundary condition $U(\mathbf{r}) \to \hat{I}_2$ as $|\mathbf{r}| \to \infty$, the configuration giving the minimal energy is the unit square matrix $U(\mathbf{r}) = \hat{I}_2$ for all $\mathbf{r}$.

The chiral symmetry of the Skyrme Lagrangian $\big(SU(2) \times SU(2)\big)/\mathbf{Z}_2 \simeq SO(4)$ is consistent with the transformation $U \to O_1 U O_2$, where $O_1$ and $O_2$ are constant matrices from the SU(2) group. The boundary condition $U(\infty) = \hat{I}_2$ spontaneously breaks this chiral symmetry and reduces it to the SO(3) symmetry that corresponds to the conjugation of $U \to OUO^\dagger$ with $O \in SU(2)$.

To establish the relation between the variables considered in this review and the variables of the pion theory using the Skyrme model, the field $U(t,\mathbf{r})$ should be written as $U = \sigma + \mathrm{i}\boldsymbol{\pi}\boldsymbol{\tau}$, where $\boldsymbol{\tau}$ is the Pauli matrix and $\boldsymbol{\pi} = (\pi_1, \pi_2, \pi_3)$ stands for the triplet of pion fields. The function $\sigma$ describes an additional field defined by the pionic field via the constraint $\sigma^2 + \boldsymbol{\pi}\boldsymbol{\pi} = 1$. This constraint arises because $U \in SU(2)$. Both the amplitude and the sign of $\sigma$ are determined by the requirement of field continuity and boundary conditions $\boldsymbol{\pi}(\infty) = 0$, $\sigma(\infty) = 1$. In terms of the pion field $\boldsymbol{\pi}$, the isospin transformation is given by $\boldsymbol{\pi} \to M\boldsymbol{\pi}$, where $M$ is the SO(3)-matrix related to $O \in SU(2)$ as

$$M_{ij} = \frac{1}{2}\,\mathrm{Tr}\,(\tau_i O \tau_j O^\dagger)\,.$$

Static $U(\mathbf{r})$ field configurations are the critical points of the functional

$$E=\frac{1}{12\pi^2}\int \mathrm{d}^3x\left\{-\frac{1}{2}\ \mathrm{Tr}\,(R_\mu R^\mu)-\frac{1}{16}\ \mathrm{Tr}\left([R_\mu,R_\nu][R^\mu,R^\nu]\right)\right\}, \tag{5.31}$$

which defines energy in the Skyrme model. For convenience, an additional factor $1/12\pi^2$ is introduced into this expression.

Taking the boundary condition into consideration, the matrix $U$ at a given time instant realizes the map $\mathsf{S}^3\mapsto\mathsf{S}^3$ that identifies the original sphere $\mathsf{S}^3$ with $\mathsf{R}^3\cup\{\infty\}$. Because the homotopy group $\pi_3(S^3)=\mathsf{Z}$ is nontrivial, the maps between three-dimensional spheres are divided into homotopy classes characterized by the integer

$$B=-\frac{1}{24\pi^2}\int \mathrm{d}^3x\,\varepsilon_{ijk}\,\mathrm{Tr}\,(R_iR_jR_k)\,, \tag{5.32}$$

which is the degree of the map $U$. The number $B$ is a topological invariant: it is conserved under continuous $U$ field deformations, including its time evolution. The conserved topological charge $B$ was identified by Skyrme with the baryon number.

The presence of a topological charge is in itself insufficient for the existence of stable static configurations because it leaves the requirement of the Derrick theorem unsatisfied [30]. Similarly to (3.1), both terms in the expression for energy (5.31), $E=E_2+E_4$, contain the second and the fourth powers of spatial derivatives of $U$. After the transformation of spatial coordinates $\mathbf{r}\to\lambda\mathbf{r}$, the expression for energy takes the form $E(\lambda)=\lambda E_2+(1/\lambda)E_4$. Because rescaling affects the two terms in opposite ways, the energy becomes minimal at a finite value $\lambda\neq 0$. This means that any distribution has a well-defined scale. It is worth noting that for any static solution, e.g., for the skyrmion representing the minimum-energy configuration in a given topological sector, $E(\mu)$ must also be minimal when $\mu=1$ and contributions to the energy from the quadratic term and the fourth-power term in derivatives are identical.

Not infrequently, the geometric description [125] of the energy of static skyrmions proves helpful. As in the nonlinear elasticity theory, the skyrmion field density energy depends on the local extension associated with the map $U\colon \mathsf{R}^3\mapsto\mathsf{S}^3$. In this approach, it is convenient to introduce the stretch tensor $D_{ij}=-(1/2)\,\mathrm{Tr}\,(R_i)R_j$ defined at each point $\mathbf{r}\in\mathsf{R}$. The expression for $D_{ij}$ is a symmetric positive definite $3\times 3$-matrix that can be regarded as a quantity describing the $U$-induced deformation. The image obtained under the action of $U$ of an infinitely small sphere with radius $\varepsilon$ centered at $\mathbf{r}\in\mathsf{R}^3$ is (in the leading order in $\varepsilon$) an ellipsoid with the main axes $\epsilon\lambda_1$, $\epsilon\lambda_2$, $\epsilon\lambda_3$, where $\lambda_1^2$, $\lambda_2^2$, and $\lambda_3^2$ are the three nonnegative eigenvalues of the matrix $D_{ij}$. The signs of $\lambda_1$, $\lambda_2$, and $\lambda_3$ are chosen such that the product $\lambda_1\lambda_2\lambda_3$ is positive (negative) if $U$ preserves (reverses) the local orientation.

In terms of these eigenvalues, the energy $E$ and the baryon number can be obtained by integration of the respective densities

$$\mathcal{E}=\frac{1}{12\pi^2}\,(\lambda_1^2+\lambda_2^2+\lambda_3^2+\lambda_1^2\lambda_2^2+\lambda_2^2\lambda_3^2+\lambda_3^2\lambda_1^2)\,, \tag{5.33}$$

$$\mathcal{B}=\frac{1}{2\pi^2}\ \lambda_1\lambda_2\lambda_3\,. \tag{5.34}$$

It follows from the inequality

$$(\lambda_1\pm\lambda_2\lambda_3)^2+(\lambda_2\pm\lambda_3\lambda_1)^2+(\lambda_3\pm\lambda_1\lambda_2)^2\geqslant 0 \tag{5.35}$$

and expression (5.33) that $\mathcal{E}\geqslant\mathcal{B}$. Therefore, the energy in the Skyrme model has the lower bound [1]

$$|E|\geqslant|B|\,. \tag{5.36}$$

It is worth noting that the Skyrme–Faddeev model in (3.1) can be derived from the Skyrme model by bounding the field by its values at the equatorial sphere $\mathsf{S}^2$ of the usual SU(2)-target space. The relation between the field $\mathbf{n}$ and the matrix $U$ has the form $U=\mathrm{i}n^a\tau^a$. Consideration of the relation between the models naturally leads to the question whether a one-parameter family of models exists that contains the Skyrme and Skyrme–Faddeev models as particular limit cases. The construction establishing the relation between these models is described below [126].

From the geometrical standpoint, we first consider the general situation with a map $\Phi$ from a three-dimensional space with coordinates $x^k$ and a metric $g^{ik}$ into another three-dimensional space with local coordinates $\varphi^a$ and a metric $H_{ab}$. The Skyrme energy density $\mathcal{E}=\mathcal{E}_2+\mathcal{E}_4$ of such a map is defined [125] in terms of the differentials $\partial_j\varphi^a$ of $\Phi$:

$$\mathcal{E}_2=g_2\,\mathrm{Tr}\,D\,,\qquad \mathcal{E}_4=\frac{1}{2}\,g_4\left[(\mathrm{Tr}\,D)^2-\mathrm{Tr}\,D^2\right], \tag{5.37}$$

where the $3\times 3$-matrix $D$ has the form

$$D_a^b=g^{jk}(\partial_j\varphi^c)\,H_{ac}(\partial_k\varphi^b)\,, \tag{5.38}$$

while $g_2$ and $g_4$ are constants.

Let the target space of the map be a three-dimensional sphere $\mathsf{S}^3$ with a one-parameter family of U(2)-invariant metrics. This family is represented by the standard SO(4)-invariant metric when the corresponding system is the usual SU(2) Skyrme model. The family of metrics can be described as follows.

Let $z=(z_1,z_2)^{\mathrm{T}}$ define, as before, a complex 2-vector subject to the relation $z^\dagger z=1$. A totality of such vectors $z$ forms the sphere $\mathsf{S}^3$. The standard metric $G$ on $\mathsf{S}^3$ corresponds to the squared interval $\mathrm{d}s^2=\mathrm{d}z^\dagger\,\mathrm{d}z$. The family of metrics parameterized by a real number $\alpha$ is constructed based on the vector field $\xi$ obtained from the 1-form $\omega=-\mathrm{i}z^\dagger\,\mathrm{d}z$ by raising its index with the help of the metric in $\mathrm{d}s^2=\mathrm{d}z^\dagger\,\mathrm{d}z$. Then, the interval for the family of metrics $H$ under consideration may assume the form

$$\mathrm{d}s^2=\mathrm{d}z^\dagger\,\mathrm{d}z+\alpha(z^\dagger\,\mathrm{d}z)(z^\dagger\,\mathrm{d}z)\,. \tag{5.39}$$

Similarly to $G$ and $\omega$, the metric $H$ is invariant under the transformations $z\to\Lambda z$, where $\Lambda\in\mathrm{U}(2)$.

If metric (5.39) is positive definite at $\alpha<1$, then, in the limit $\alpha=0$, it becomes degenerate and, at $\alpha=1$, becomes the standard metric on $\mathrm{CP}^1\simeq\mathsf{S}^2$. In other words, the one-parameter family being considered includes the standard sphere $\mathsf{S}^3$ at $\alpha=0$ and the standard sphere $\mathsf{S}^2$ at $\alpha=1$. Therefore, the values of $\alpha$ from the range $0\leqslant\alpha\leqslant 1$ describe the interpolation between the Skyrme and Skyrme–Faddeev systems.

We consider [126] the Lagrangian $\mathcal{L}$ of the generalized Skyrme model compatible with expression (5.31) for the

energy density of static configurations. Let a vector $z$ define the SU(2) matrix as

$$U = \begin{pmatrix} z^1 & -z^{*2} \\ z^2 & z^{*1} \end{pmatrix}. \tag{5.40}$$

In terms of the current density $L_\mu = \mathrm{i}L^a_\mu \tau_a = U^\dagger \partial_\mu U$ satisfying the commutation relation $[L_\mu, L_\nu] = K_{\mu\nu} = \mathrm{i}K^a_{\mu\nu}\tau^a$ (with the Pauli matrices $\tau^a$), the Lagrangian is

$$\mathcal{L} = \mathcal{L}_2 + \mathcal{L}_4\,,$$

where

$$\mathcal{L}_2 = g_2 g^{\mu\nu}(L^a_\mu L^a_\nu - \alpha L^3_\mu L^3_\nu)\,, \tag{5.41}$$

$$\mathcal{L}_4 = \frac{1}{8}\, g_4 g^{\mu\nu} g^{\beta\gamma}\left[(1-\alpha)K^a_{\mu\beta}K^a_{\nu\gamma} + \alpha K^3_{\mu\beta}K^3_{\nu\gamma}\right]. \tag{5.42}$$

The global U(2) symmetry with a parameter $\theta$ corresponds to the transformation $U \mapsto \Omega U \Gamma$, where $\Gamma$ is an SU(2) matrix and $\Omega = \exp(\mathrm{i}\theta\sigma_3)$ is the diagonal SU(2) matrix preserving $L^a_\mu L^a_\nu$ and $L^3_\mu$.

The case of $\alpha = 1$ yields the Skyrme–Faddeev Lagrangian. One way to see this is to substitute the field $z$ by the unit vector field $n^a = z^\dagger \tau^a z$. Then, the Lagrangian $\mathcal{L}$ at $\alpha = 1$ is equal to

$$\mathcal{L} = \frac{1}{4}\, g_2(\partial_\mu \mathbf{n})^2 + \frac{1}{32}\, g_4\big(\mathbf{n}\,[\partial_\mu \mathbf{n} \times \partial_\nu \mathbf{n}]\big)^2\,, \tag{5.43}$$

i.e., is the Skyrme–Faddeev Lagrangian.

Fields with a finite energy satisfy the boundary condition $U \to U_0$ as $r \to \infty$, where $U_0$ is a constant matrix. These fields are classified topologically based on the winding number $B = \int \mathcal{B}\,\mathrm{d}^3x$, where $\mathcal{B} = \varepsilon_{ikl}\,\mathrm{Tr}\,(L_i L_k L_l)/(24\pi^2)$. In the limit $\alpha \to 1$, number $B$ equals the Hopf invariant $Q$ for $\mathsf{S}^2$-valued $\mathbf{n}$ fields.

As emphasized earlier, constant values are consistent with the choice of the scale for measuring the length and the energy. For convenience, we can consider the field $z(x^k)$ corresponding to the identical map of the sphere $\mathsf{S}^3$ onto itself. The energy of this field is $E = 2\pi^2\big[(3-\alpha)g_2 + (3-2\alpha)g_4\big]$ [126]. Under the assumptions that $g_2 = 1/\big[4\pi^2(3-\alpha)\big]$ and $g_4 = 1/\big[4\pi^2(3-2\alpha)\big]$, the field $z(x^k)$ has the energy $E = 1$ at any $\alpha \in [0,1]$. The family of Skyrme solutions from this interval at different values of $B$ was considered in more detail in Ref. [126].

### 5.4 Polyakov holonomy

The discussion of the association between knotted configurations and instantons is convenient to begin from the analysis of an auxiliary problem of obtaining a skyrmion field from Yang–Mills instantons. The interrelation between the Skyrme and Skyrme–Faddeev models considered in Section 5.3 may be helpful in answering the main question.

The scheme for obtaining Skyrme fields from instantons includes [123] the calculation of the Polyakov exponential, i.e., holonomy of SU(2) instanton fields along the $x^4$ axis in the Euclidean space $\mathsf{R}^4$:

$$U(\mathbf{r}) = \mathcal{T}\exp\int_{-\infty}^{+\infty} A_4(\mathbf{r}, x^4)\,\mathrm{d}x^4\,, \tag{5.44}$$

where $\mathcal{T}$ denotes time-ordering and $A_\mu$ is the Yang–Mills instanton field potential in $\mathsf{R}^4$. The component $A_4$ of the potential taking values in the SU(2) algebra, its exponential has values in the SU(2) group; thus, $U(\mathbf{r})$ realizes a map $\mathsf{R}^3 \mapsto \mathrm{SU}(2)$ as required for the static Skyrme field.

When scrutinizing the problem more thoroughly, one needs to suppose that both integration limits, $-\infty$ and $+\infty$, refer to one point in $\mathsf{S}^4$ corresponding to a point at infinity in $\mathsf{R}^4$. Then, the holonomy is taken along a closed loop in $\mathsf{S}^4$ and is almost gauge invariant. The residual action of the gauge transformation $g(x)$ consists of a similarity transformation of $U(\mathbf{r})$ with the constant element $g(\infty)$. This corresponds to a certain isospin rotation of the Skyrme field. The boundary condition $U \to I_2$ at $|\mathbf{r}| \to \infty$ is satisfied in this scheme because the loop size in $\mathsf{S}^4$ tends to zero in this limit.

When considering calculations in a practical context, it should be remembered that the requirement that holonomy be taken along a closed curve implies that an additional factor in the form of a transition function that sends the point $+\infty$ back to $-\infty$ must be included in (5.44). For an instanton in the 't Hooft ansatz [127], expression (5.44) is complete, whereas in the ansatz [128], an additional factor $-1$ is needed. In the axial gauge, when $A_4 = 0$, the holonomy is entirely contained in the transition function at infinity.

Generally speaking, there is no need to use instanton configurations of the Yang–Mills field, expression (5.44) remaining valid for an arbitrary field $A_\mu$. However, if the consideration is confined to instantons, the result is a large and finite-dimensional family of the Skyrme fields $U$. Such fields are not exact solutions of the equations of motion in the Skyrme model, but some of them can fairly well approximate the Skyrme distributions with minimal energy.

If the potential $A_\mu$ is a self-dual Yang–Mills field with the instanton charge $N$, i.e., with the Pontryagin index

$$N = \frac{1}{8\pi^2}\int \mathrm{Tr}\,(F^*_{\mu\nu}F_{\mu\nu})\,\mathrm{d}^4x\,,$$

where $F^*_{\mu\nu} = (1/2)\varepsilon_{\mu\nu\alpha\beta}F_{\alpha\beta}$, then the resulting Skyrme field has the baryon number $B = N$. This inference can be verified by specific examples while the general result comes from continuity. In terms of $N$, the construction permits obtaining the $(8N-1)$-dimensional family of Skyrme fields from the $8N$-dimensional instanton family with charge $N$. One parameter is lost because instanton translation in the direction of $x^4$ does not change the Skyrme field due to the integration over $x^4$.

Regarded as the main example, the instanton with charge 1 given by the 't Hooft ansatz

$$\rho(x) = 1 + \frac{\lambda^2}{|x-a|^2}$$

[with $A_\mu = (\mathrm{i}/2)\tau_{\mu\nu}\partial_\nu \log\rho$] with scale $\lambda$ and coordinates of the center $a = 0$ generates the Skyrme field in a 'hedgehog' form: $U(\mathbf{r}) = \exp\{\mathrm{i}f(r)n^a\tau^a\}$ or $\pi^a = n^a\cos f(r)$ and $\sigma = \sin f(r)$, with the function

$$f(r) = \pi\left[1 - \left(1 + \frac{\lambda^2}{r^2}\right)^{-1/2}\right].$$

Instantons are gauge invariant. Therefore, the arbitrary parameter $\lambda$ may be chosen such that it minimizes the energy of the resultant Skyrme field. The corresponding scale and

energy values are $\lambda^2 = 2.11$ and $E = 1/243$. The latter value is only 1% higher than the energy of the true skyrmion solution.

The main difficulty arising in this construction consists of the computation of holonomy because the integration in (5.44) is path-ordered. To calculate the path-ordered exponential (5.44), it is necessary to introduce a quantity $\hat{U}(\mathbf{r}, x^4)$ and solve the matrix ordinary differential equation $\partial\hat{U}/\partial x^4 = A_4\hat{U}$ along the real line $x^4 \in (-\infty, \infty)$ with the coordinate $\mathbf{r}$ considered a parameter and with the initial condition $\hat{U}(\mathbf{r}, -\infty) = \hat{I}_2$. The Skyrme field $U(\mathbf{r})$ can then be obtained at the end-point of the $x^4$-flow: $U(\mathbf{r}) = \hat{U}(\mathbf{r}, \infty)$.

After the detailed discussion of the procedure for constructing the basic solution in the problem of the relation between the Skyrme configuration and instantons, it is easy to see specific features of the construction establishing the place of instantons in the Skyrme – Faddeev problem. To have an approximate knotted configuration with the Hopf invariant $Q$, one only needs to apply [128] the standard Hopf map [see (4.1)] to the approximate Skyrme configurations.

Let $X^\mu = (t, x^j)$ denote coordinates in the Euclidean space $\mathsf{R}^4$ and $A_\mu$ be the SU(2) gauge potential in $\mathsf{R}^4$ with a topological charge $N$. Furthermore, for a fixed point with coordinates $x^j \in \mathsf{R}^3$, let a function $U(x^j)$ [i.e., Polyakov's exponential (5.44)] be a Skyrme configuration with values in the SU(2) gauge group. The use of the Hopf map from $\mathsf{S}^3$ to $\mathsf{S}^2$ at this step yields the $\mathsf{S}^2$-valued field $\mathbf{n}(x^j)$. Specifically, the $2 \times 2$-matrix $U_{ab}(x^j)$ is used in the expression for the stereographic projection

$$W(x^j) = \frac{n_1 + \mathrm{i}n_2}{1 + n_3}\,, \tag{5.45}$$

under the assumption that $W(x^j) = U_{21}(x^j)/U_{11}(x^j)$. With the appropriately decreasing gauge potential $A_\mu$ at $|X| \to \infty$ (as is the case in the forthcoming discussion), the function $W(x^j)$ satisfies the required boundary condition $W(x^j) \to 0$ as $r \to 0$, and its Hopf invariant equals $N$.

The energy of a skyrmion system is invariant under isospin transformations $U \mapsto \Lambda^{-1}U\Lambda$, where $\Lambda \in \mathrm{SU}(2)$ is a constant matrix. Such $\Lambda$ provide three additional parameters that do not affect the energy in the skyrmion case. Both $\Lambda$ and $-\Lambda$ defining the same transformation, this parameter space is SO(3). However, the Hopf map breaks the symmetry. Therefore, in the general case, a transformation $U \mapsto \Lambda^{-1}U\Lambda$ is essential as, for example, for $N = 2$ [29].

The above construction holds for any gauge field. However, its main advantage is the use of instantons leading to highly significant configurations. Suffice it to say that instantons may be regarded in this context as configurations that interpolate between different knotted vacuum configurations of the field $\mathbf{n}$. There is a simple formula (cf. [129]) for the instanton solutions at $N = 1, 2$ when $A_4$ has the form

$$A_4 = \frac{\mathrm{i}}{2}\,\Omega^{-1}(\partial_j\Omega)\tau_j\,, \tag{5.46}$$

where

$$\Omega(X) = \sum_{a=1}^{N+1} \frac{\lambda_a^2}{|X - X_a|^2}\,. \tag{5.47}$$

Here, $X_a$ denotes the coordinates of different points in $\mathsf{R}^4$. Although $A_4$ has poles at these points, the poles can be removed. Then, the $\mathbf{n}(x^\mu)$ configuration is a smooth function in $\mathsf{R}^3$. This ansatz yields the $N$-instanton solution for any $N \geqslant 1$ and gives all instantons in the corresponding topological sectors at $N = 1$ and $N = 2$.

We consider the sector with $N = 1$ for simplicity. The special limit $\lambda_2 = |X_2| \to \infty$ in expression (5.47) gives the 't Hooft function

$$\Omega(X) = 1 + \frac{\lambda_1^2}{|X - X_1|^2}\,. \tag{5.48}$$

The function $\Omega(X)$ depends on five real parameters $(\lambda_1, X_1^\mu)$. Because we integrate over $t$, it may be assumed, without the loss of generality, that $t_1 = 0$. Having the solution at the center of the three-dimensional space, we are left with a single parameter, the scale factor $\lambda$. In this case, holonomy can be calculated analytically [123], yielding the Hopf configuration

$$W = \frac{x + \mathrm{i}y}{z - \mathrm{i}r\cot f(r)} \tag{5.49}$$

with the function

$$f(r) = \pi\left[1 - \frac{r}{\sqrt{r^2 + \lambda^2}}\right]. \tag{5.50}$$

Expressions (5.49) and (5.50) give a one-parameter family of linked configurations analogous to the 'hedgehog' configuration in the Skyrme model. With an appropriate choice of coupling constants, the energy is the same functional of $f$ in both systems. It is already known from the consideration of the Skyrme model (cf. [123, 130]) that the configuration energy $E(\lambda) = 0.428\lambda + 0.903/\lambda$ has the minimum value $E = 1.243$ at $\lambda = 1.45$. The case of axially symmetric distributions at $N = 0$ is discussed at greater length in Ref. [29].

### 5.5 The dual picture

In (5.8), in considering a particular case of relation (5.3) for clarity, we factored out one scalar degree of freedom and the $\mathbf{n}$-field-associated degrees of freedom having a magnetic interpretation. In the present section, based on the results in Refs [131, 132], we discuss the factorization in the general situation with a duality between 'magnetic' and 'electric' variables in the Yang – Mills theory at large distances. The decomposition of the degrees of freedom proposed in Ref. [131], which includes the Abelian scalar multiplet with two complex scalar fields, besides the univector field, allows the natural electrical interpretation. Magnetic variables give a relativistic version of the Heisenberg model. Such a factorization realizes the symmetry between electric and magnetic variables and leads to a dual picture for the corresponding phases of the theory. In this case, factorization of the degrees of freedom proves to be consistent with the fact that the physical spectrum of states of the theory contains confining strings arranged into stable knotted solitons.

Decomposition (5.3) [94, 95] entails the necessity of using the unit magnetic vector field. However, string-like excitations of gauge theory must correspond to variables with the electric interpretation [105, 104]. This explains why a new ansatz differing from (5.3) is introduced in Ref. [131] to represent the gauge field. The variant of the decomposition proposed in [131] contains two different unit vector fields. These variables enter the action in a symmetric way such that their introduction leads to a dual picture.

The substitution of independent variables in the case of the four-dimensional SU(2) Yang–Mills theory (when using compact variables) leads to structures of type (5.1) and includes the following steps [131]. In the maximally Abelian gauge [105, 106], the Cartan component $A_\mu^3$ of the SU(2) field behaves as an Abelian gauge field, whereas the field $A_\mu^+ = A_\mu^1 + \mathrm{i}A_\mu^2$, together with its complex-conjugate partner, behaves under the Abelian gauge transformations as charged vector fields do. Two vector near-diagonal fields $A_\mu^1$ and $A_\mu^2$ determine the two-dimensional plane in the four-dimensional Euclidean space–time. This plane must be parameterized with the help of vectors $e^a{}_\mu$, $a = 1, 2$ that satisfy the ortonormalization conditions $e^a{}_\mu e^b{}_\mu = \delta^{ab}$ and define a basis in the plane.

When using the variables $e^a{}_\mu$, the degrees of freedom in the components of $A_\mu^a$ may be factored as

$$A_\mu^a = M^a{}_b e^b{}_\mu . \tag{5.51}$$

Two near-diagonal components of the potential $A_\mu^a$ describe eight degrees of freedom. The right-hand side of (5.51) contains nine degrees of freedom because the matrix $M^a{}_b$ has four independent components and the two normalized vectors $e^a{}_\mu$ have five independent components. However, there is also the internal SO(2) $\sim$ U(1) rotational invariance between $M^a{}_b$ and $e^a{}_\mu$. Namely, if the vectors $e^a{}_\mu$ at a fixed value of the index $\mu$ are rotated as $e^a{}_\mu \to \mathcal{O}^a{}_b e^b{}_\mu$, decomposition (5.51) remains unaltered under the $M^a{}_b$ transformation from the right with the help of the same matrix $\mathcal{O}^a{}_b$. This gauge invariance being taken into account, the right-hand side of expression (5.51) actually contains eight independent field degrees of freedom.

By introducing the combination

$$\mathbf{e}_\mu = \frac{1}{\sqrt{2}} (e^1{}_\mu + \mathrm{i}e^2{}_\mu) , \tag{5.52}$$

which satisfies the conditions

$$\mathbf{e}^2 = 0 , \qquad \mathbf{e}\mathbf{e}^+ = 1 , \tag{5.53}$$

the factored degrees of freedom in (5.51) may be represented as

$$A_\mu^1 + \mathrm{i}A_\mu^2 = \mathrm{i}\psi_1 \mathbf{e}_\mu + \mathrm{i}\psi_2 \mathbf{e}_\mu^+ . \tag{5.54}$$

Here, the four matrix elements $M^a{}_b$ are redistributed into two complex scalar fields $\psi_1$ and $\psi_2$.

The diagonal SU(2) gage transformation leads to

$$A_\mu^3 \equiv A_\mu \to A_\mu - \partial_\mu \xi , \tag{5.55}$$

with both fields $\psi_1$ and $\psi_2$ multiplied by the common phase,

$$\psi_{1,2} \to \exp(\mathrm{i}\xi)\, \psi_{1,2} , \tag{5.56}$$

while $e^a{}_\mu$ remains unaltered. These expressions describe the usual electric Abelian gauge transformation with the electrically charged $\psi_{1,2}$ fields.

On the other hand, internal U(1) rotations lead to

$$\mathbf{e}_\mu \to \exp(-\mathrm{i}\zeta)\, \mathbf{e}_\mu \tag{5.57}$$

and

$$\psi_1 \to \exp(\mathrm{i}\zeta)\, \psi_1 , \qquad \psi_2 \to \exp(-\mathrm{i}\zeta)\, \psi_2 . \tag{5.58}$$

In this case, the decomposition is unaffected and the composite vector field

$$C_\mu = \mathrm{i}\mathbf{e}\, \partial_\mu \mathbf{e}^+ \tag{5.59}$$

undergoes a transformation according to the law

$$C_\mu \to C_\mu - \partial_\mu \zeta . \tag{5.60}$$

For this reason, $C_\mu$ may be regarded as a gauge field for internal rotations. Specifically, transformation (5.60) may be interpreted as an axial or magnetic U(1) gauge transformation.

The real antisymmetric tensor

$$G_{\mu\nu} = \mathrm{i}(\mathbf{e}_\mu \mathbf{e}_\nu^+ - \mathbf{e}_\nu \mathbf{e}_\mu^+) , \tag{5.61}$$

constructed with the help of complex vector (5.52) is invariant under electric and magnetic transformations. Its use allows introducing electric and magnetic combinations of the form

$$\mathcal{E}_k = G_{k0} , \qquad \mathcal{B}_k = \frac{1}{2}\, \varepsilon_{klm} G_{lm} . \tag{5.62}$$

In the approach proposed in Ref. [131], the two fields

$$\mathbf{u} = \vec{\mathcal{E}} + \vec{\mathcal{B}} , \qquad \mathbf{v} = \vec{\mathcal{E}} - \vec{\mathcal{B}} \tag{5.63}$$

are independent three-component unit vectors. Taking (5.61) into consideration, $\mathbf{e}_\mu$ can be expressed via the $\mathbf{u}$ and $\mathbf{v}$ vectors as

$$\mathbf{e}_\mu = \frac{\exp(\mathrm{i}\phi)}{\sqrt{2}} \left( e_0, \frac{1}{2e_0} \{ \mathbf{u} \times \mathbf{v} + \mathrm{i}(\mathbf{u} + \mathbf{v}) \} \right) , \tag{5.64}$$

where $\phi$ is the phase of the $\mathbf{e}_\mu$ field zeroth component. The normalization condition (5.53) gives $e_0 = \sqrt{1 + \mathbf{u}\mathbf{v}}$ for the modulus. Magnetic gauge field (5.59) expressed through the unit vectors $\mathbf{u}$ and $\mathbf{v}$ acquires the form

$$C_\mu = \frac{1}{1 + \mathbf{u}\mathbf{v}} (\partial_\mu \mathbf{u} + \partial_\mu \mathbf{v})\, [\mathbf{u} \times \mathbf{v}] + 2\partial_\mu \phi , \tag{5.65}$$

which identifies $\phi$ as a magnetic phase.

To write the Yang–Mills Lagrangian in new terms, we define two complex vectors

$$U_\mu = \exp(\mathrm{i}\phi)\, \frac{\partial_\mu \mathbf{u} \left( \mathbf{v} + \mathrm{i}[\mathbf{u} \times \mathbf{v}] \right)}{\sqrt{1 - (\mathbf{u}\mathbf{v})^2}} , \tag{5.66}$$

$$V_\mu = \exp(\mathrm{i}\phi)\, \frac{\partial_\mu \mathbf{v} \left( \mathbf{u} + \mathrm{i}[\mathbf{u} \times \mathbf{v}] \right)}{\sqrt{1 - (\mathbf{u}\mathbf{v})^2}} \tag{5.67}$$

and, assuming that $\rho^2 = |\psi|^2$, the three-component unit vector

$$\mathbf{t} = \frac{1}{\rho^2} (\psi_1^*, \psi_2^*)\, \boldsymbol{\sigma} \begin{pmatrix} \psi_1 \\ \psi_2 \end{pmatrix} . \tag{5.68}$$

This vector is invariant under electric gauge transformation (5.56). Moreover, the component $t_3$ is invariant under the magnetic gauge transformation, while the other two compo-

nents transform as

$$t_{\pm} = \frac{1}{2}(t_1 \pm \mathrm{i}t_2) \to \exp(\mp 2\mathrm{i}\xi)\, t_{\pm}\,. \tag{5.69}$$

Using the above variables and definitions and following [131], we rewrite the Yang–Mills Lagrangian with a partly fixed gauge [104, 105] for the near-diagonal components $A_\mu^a$ with respect to the diagonal Cartan components $A_\mu \equiv A_\mu^3$ of the gauge field as

$$\mathcal{L} = \frac{1}{4}(F_{\mu\nu}^a)^2 + \frac{1}{2}\left[(\partial_\mu \delta^{ab} - \varepsilon^{ab} A_\mu) A_\mu^b\right]^2, \tag{5.70}$$

where $F_{\mu\nu} = \partial_\mu A_\nu - \partial_\mu A_\nu$. Substituting the gauge field written in the new variables in Eqn (5.70) gives the following expression for the gauge-fixed Lagrangian

$$\begin{aligned}
&\mathcal{L} = \mathcal{L}_1 + \mathcal{L}_2 + \mathcal{L}_3\,,\\
&\mathcal{L}_1 = \frac{1}{4}\,F_{\mu\nu}^2 + |D_\mu^{ab}\psi_b|^2 + \frac{1}{8}\left(|\psi_1|^2 - |\psi_2|^2\right)^2, \qquad (5.71)\\
&\mathcal{L}_2 = \frac{1}{2}\,\rho^2\left(|\partial_\mu \mathbf{u}|^2 + |\partial_\mu \mathbf{v}|^2\right) + \frac{1}{2}\,\rho^2 t_- U_\mu V_\mu + \frac{1}{2}\,\rho^2 t_+ U_\mu^* V_\mu^*\,, \qquad (5.72)\\
&\mathcal{L}_3 = \frac{1}{2}\,\rho^2 t_3 F_{\mu\nu} G_{\mu\nu}\,. \qquad (5.73)
\end{aligned}$$

Expressions (5.71)–(5.73) should be supplemented by the Lagrangian for ghosts necessary to compute radiation corrections. In representation (5.71), $D_\mu^{ab} = \delta^{ab}(\partial_\mu + \mathrm{i}A_\mu) - \mathrm{i}\sigma_3^{ab} C_\mu$ is a U(1) × U(1)-covariant variable. Indeed, expressions (5.71)–(5,73) are invariant with respect to both the electric U(1) gauge group and the internal magnetic U(1) group.

We introduce the vector field

$$B_\mu = A_\mu + \frac{\mathrm{i}}{2\rho^2}\left[\psi_a \hat{D}_\mu^{ab} \bar{\psi}_b - \bar{\psi}_a \hat{D}_\mu^{ab} \psi_b\right] \equiv A_\mu + \frac{\mathrm{i}}{2\rho^2}\, J_\mu\,, \tag{5.74}$$

where $\hat{D}^{ab} = \delta_{ab}\partial_\mu - \mathrm{i}\sigma_3^{ab} C_\mu$ is the magnetic covariant derivative, which is therefore equal to $D_\mu^{ab}$ with the field $A_\mu$ eliminated. Then, the $B_\mu$ field is invariant under the electric U(1) gauge transformation.

Using definition (5.74), the electric U(1) gauge structure can be removed from Eqns (5.71)–(5.73) by writing the Lagrangian in terms of manifestly invariant quantities $B_\mu$ and $\mathbf{t}$ as [131]

$$\begin{aligned}
&\mathcal{L} = \mathcal{L}_1' + \mathcal{L}_2'\,,\\
&\mathcal{L}_1' = \frac{1}{4}(H_{\mu\nu} + M_{\mu\nu} + K_{\mu\nu} t_3)^2 + \frac{1}{2}(\partial_\mu \rho)^2 + \rho^2 (\nabla_\mu^{ij} t_j)^2\\
&\qquad + \rho^2 B_\mu^2 + \frac{1}{8}\,\rho^4 t_3^2\,, \qquad (5.75)\\
&\mathcal{L}_2' = \frac{1}{2}\,\rho^2\left(|\partial_\mu \mathbf{u}|^2 + |\partial_\mu \mathbf{v}|^2\right) + \frac{1}{2}\,\rho^2\left(t_- U_\mu V_\mu + t_+ U_\mu^* V_\mu^*\right.\\
&\qquad \left. + t_3[H_{\mu\nu} + M_{\mu\nu} + K_{\mu\nu} t_3] G_{\mu\nu}\right), \qquad (5.76)
\end{aligned}$$

where

$$\nabla_\mu^{ij} = \delta^{ij}\partial_\mu + 2\varepsilon^{ij3} C_\mu \tag{5.77}$$

defines the action of the magnetic covariant variable on a vector and

$$\begin{aligned}
&H_{\mu\nu} = \partial_\mu B_\nu - \partial_\nu B_\mu\,, \qquad (5.78)\\
&M_{\mu\nu} = \varepsilon^{ijk} t_i \nabla_\mu^{jl} t_l \nabla_\nu^{km} t_m\,, \qquad (5.79)\\
&K_{\mu\nu} = \partial_\mu C_\nu - \partial_\nu C_\mu\,. \qquad (5.80)
\end{aligned}$$

The dual structure in (5.75) and (5.76) expressed in terms of the electric $\mathbf{t}$ and magnetic $\mathbf{u}$ and $\mathbf{v}$ variables becomes especially clear if the consideration is confined to the static configurations in the ground state described by the Hamiltonian

$$\begin{aligned}
&H = H_1 + H_2\,,\\
&H_1 = \frac{1}{4}(H_{ij} + M_{ij} + K_{ij} t_3)^2 + \frac{1}{2}(\partial_i \rho)^2 + \rho^2 (\nabla_i \mathbf{t})^2\\
&\qquad + \rho^2 B_i^2 + \frac{1}{8}\,\rho^4 t_3^2\,, \qquad (5.81)\\
&H_2 = \frac{1}{2}\,\rho^2 |\partial_i \mathbf{m}|^2\\
&\qquad + \frac{1}{2}\,\rho^2\left(t_+ Q_i^2 + t_- \bar{Q}_i^2 + t_3 \varepsilon_{ijk} m_i [H_{jk} + M_{jk} + K_{jk} t_3]\right), \qquad (5.82)
\end{aligned}$$

where $\mathbf{m}$ is a three-component unit vector taking real values, whose components are equal to $m_i = -(\mathrm{i}/2)\varepsilon_{ijk} G_{jk}$ in the static limit. Besides (5.59), there is an additional component vector $Q_i = \mathrm{i}\mathbf{m}\,\partial_i \mathbf{e}$ together with its complex-conjugate partner. These vector fields are charged, $Q_i \to \exp(\mathrm{i}\xi) Q_i$, with respect to the magnetic gauge transformations but remain covariant under the electric gauge transformations. In the static case $\mathbf{m} = \mathbf{u} = \mathbf{v}$, $Q_i = U_i = V_i$. In this limit, the total rotation group SO(4) = SU(2) × SU(2) in the Euclidean space reduces to the spatial rotation group SO(3). Moreover, in the static limit, $K_{ij} = \mathbf{m}\,[\partial_i \mathbf{m} \times \partial_j \mathbf{m}]$.

Expressions (5.75) and (5.76) or (5.81) and (5.82) resemble (2.3) in many respects, including the potential term. For the vector field $\mathbf{t}$, the following expression for the potential energy ensues from (5.75) and (5.76):

$$V(\mathbf{t}) = \frac{1}{8}\,\rho^4 t_3^2 + \frac{1}{2}\,\rho^2\left(t_- U_\mu V_\mu + t_+ U_\mu^* V_\mu^* + t_3[H_{\mu\nu} + M_{\mu\nu} + K_{\mu\nu} t_3] G_{\mu\nu}\right). \tag{5.83}$$

The same refers to the potential term for the vector $\mathbf{m}$:

$$V(\mathbf{m}) = \varepsilon_{ijk} m_i [H_{jk} + M_{jk} + K_{jk} t_3]\, t_3\,. \tag{5.84}$$

Although these expressions look like the terms breaking the global SO(3) rotational invariance of the subsystems associated with vector fields $\mathbf{t}$ and $\mathbf{m}$, there is the manifest SO(3)-covariance.

The logarithmic corrections in the one-loop approximation result in the function $\rho^2$ acquiring a nontrivial nonzero mean value $\langle \rho^2 \rangle = \Lambda^2$ in the ground state, meaning that the last two terms in expression (5.75) are responsible for the vector fields $B_\mu$ and $\mathbf{t}$ becoming massive. Further studies of the properties of Lagrangian (5.75), (5.76) require the use of gradient expansion in which one of the variables is first regarded as 'slow' and as determining the background; thereafter, the response of the remaining 'fast' variables is evaluated in this background.

Let the electric variable $\mathbf{t}$ in this Born–Oppenheimer approach change rapidly in the background of slow magnetic variables. Taking the rotational symmetry in the four-dimensional Euclidean space into consideration, it is natural to set $\langle \mathbf{u} \rangle = \langle \mathbf{v} \rangle = 0$. This accounts for the disappearance of terms linear in $\mathbf{u}$ and $\mathbf{v}$ in the zeroth approximation and the simplification of Lagrangian (5.75), (5.76) to the expression

$$\mathcal{L} \approx \frac{1}{4}(H_{\mu\nu} + \mathbf{t}\,\partial_\mu \mathbf{t} \times \partial_\nu \mathbf{t})^2 + \Lambda^2(\partial_\mu \mathbf{t})^2 + \Lambda^2 B_\mu^2 + \frac{1}{8}\Lambda^4 t_3^2 + \frac{1}{2}\Lambda^2(t_+ S_+ + t_- S_-)\,, \tag{5.85}$$

where

$$S_+ = \langle \partial_\mu \mathbf{e}\, \partial_\mu \mathbf{e} \rangle\,. \tag{5.86}$$

It can be seen that expression (5.85) describes the dynamics of the unit vector field $\mathbf{t}$ coupled to the massive vector field $B_\mu$. The potential term is a combination of the mass $t_3$-term and the analog of the external magnetic field acting on components $t_\pm$. Such terms are always present at $\Lambda^2 \neq 0$; the background associated with the field $\mathbf{e}_\mu$ is not necessarily homogeneous. Also, it is worth noting that expression (5.85) essentially supports the hypothesis according to which the electrical phase of the SU(2) Yang–Mills theory in the infrared limit describes the dynamics of massive knotted solitons.

The structure associated with the unit vector field also arises from the Born–Oppenheimer approximation for dual magnetic variables regarded as fast variables in the background of slowly changing electric variables. In the zeroth order, averaging the Lagrangian over $\mathbf{t}$ under the condition that $\langle \mathbf{t} \rangle = 0$ and $\langle t_1^2 \rangle = \langle t_2^2 \rangle = \langle t_3^2 \rangle = 1/3$ yields [131]

$$\mathcal{L} \approx \frac{1}{4} K_{\mu\nu}^2 + \frac{1}{12} H_{\mu\nu}^2 + \Lambda^2 B_\mu^2 + \frac{1}{2}\Lambda^2\big(|\partial_\mu \mathbf{u}|^2 + |\partial_\mu \mathbf{v}|^2\big) + \frac{1}{6}\Lambda^2 K_{\mu\nu} G_{\mu\nu}\,. \tag{5.87}$$

If expression (5.87) is confined to static configurations, the Hamiltonian takes the form

$$H = \Lambda^2(\partial_i \mathbf{m})^2 + \frac{1}{4}(\mathbf{m}\,\partial_i \mathbf{m} \times \partial_j \mathbf{m})^2 + \frac{1}{12} H_{ij}^2 + \Lambda^2 B_i^2 + \frac{1}{6}\Lambda^2 m_i \varepsilon_{ijk} \langle K_{jk} \rangle\,. \tag{5.88}$$

It can be seen that the exact global SO(3) symmetry is broken when the background analog of the external magnetic field $\varepsilon_{ijk} K_{jk}$ is nontrivial. The potential term once again removes the massless states from the spectrum. Also, comparison with (5.85) reveals an obvious duality between the electric and magnetic variables. In particular, both sets of variables lead to the description containing massive knotted solitons in the spectrum.

### 5.6 Certain peculiarities of SU(3) fields

One of the main results in Ref. [131] considered in Section 5.5 is the proof that after a change of variables, the Lagrangian of the SU(2) Yang–Mills field in different phase states contains structures of the form $\mathcal{L}_1 = (\partial_\mu \mathbf{n})^2$ and $\mathcal{L}_2 = \big(\mathbf{n}\,[\partial_\mu \mathbf{n} \times \partial_\nu \mathbf{n}]\big)^2$. Their joint contribution leads to solutions in the form of stable string-like solitons. The study in [131] was motivated by the assumption that such excitations survive in the complete Yang–Mills theory. A natural question arising in this approach is how to generalize the field $\mathbf{n}$ and the structure $\mathcal{L}_1 + \mathcal{L}_2$ to higher-rank groups, e.g., to the SU(3) group, of importance in quantum chromodynamics. Such a problem was considered in Refs [132, 133].

One result in [132, 133] was the finding that duality of the SU(2) gauge field cannot be directly translated into the case of a higher-rank group, the reason being that the Lagrangian for 'electric' variables proves to be more tightly involved in the change of SU(3) Yang–Mills field parameterization compared with the Lagrangian for 'magnetic' variables. This leads to the appearance of the 'electric' variables having no 'magnetic' partners. It turns out that under reparameterizations, the SU(3) Lagrangian, unlike the Lagrangian of the SU(2) Yang–Mills field, is not invariant under the $A_\mu^a \to -A_\mu^a$ transformation of its non-Cartan components with the index $a \neq 3, 8$. This accounts for the appearance of additional 'electric' angular variables in the Lagrangian.

The SU(3) generalization of the dual parameterization of the Yang–Mills field proposed in Ref. [132] permits expressing the Lagrangian of the SU(3) theory through three neutral scalar fields $\rho_a$, two massive vector fields, three complex unit-length vectors $\mathbf{e}_\mu^a$ allowing magnetic interpretation, and seven angular electric variables.

In the case of the direct product of subgroups $\mathrm{SU}(2)^{\otimes 3}$ discussed above, the Lagrangian for the 'electric' unit vectors $t^a$ $(a = 1, 2, 3)$ defined by angular variables has the following form upon gradient expansion [132]:

$$\mathcal{L}_\mathrm{e} = \mathcal{L}_{\mathrm{e}1} + \mathcal{L}_{\mathrm{e}2}\,,$$

$$\mathcal{L}_{\mathrm{e}1} = \frac{1}{12}\left(\sum_{a=1}^{3}\Big(\big(\mathbf{t}^a\,[\partial_\mu \mathbf{t}^a \times \partial_\nu \mathbf{t}^a]\big) - \tilde{\rho}_a^2 \sum_{b=1}^{3}\big(\mathbf{t}^b\,[\partial_\mu \mathbf{t}^b \times \partial_\nu \mathbf{t}^b]\big)\Big)^2 + \sum_{a=1}^{3}\rho_a^2(\partial_\mu \mathbf{t}^a)^2\right), \tag{5.89}$$

$$\mathcal{L}_{\mathrm{e}2} = \frac{1}{12}\left(\frac{s_3}{s_2}\left(\sum_{a=1}^{3}\frac{[\partial_\mu \mathbf{t}^a \times \mathbf{t}^a]_3\, t_3^a}{4\big(1-(t_3^a)^2\big)} + 3\partial_\mu \omega^a\right)^2 + V(\mathbf{t}^1, \mathbf{t}^2, \mathbf{t}^3)\right), \tag{5.90}$$

where

$$\rho_a^2 \equiv A_\nu^a \bar{A}_\nu^a\,, \qquad \tilde{\rho}_a^2 = \prod_{b \neq a} \frac{\rho_b^2}{\rho_1^2\rho_2^2 + \rho_1^2\rho_3^2 + \rho_2^2\rho_3^2}\,,$$

$$\frac{s_3}{s_2} = \frac{\rho_1^2\rho_2^2\rho_3^2}{\rho_1^2\rho_2^2 + \rho_1^2\rho_3^2 + \rho_2^2\rho_3^2}\,,$$

where the 1-form defining the angular variable $\omega^a$ is one of the aforementioned variables, and $V(\mathbf{t}^1, \mathbf{t}^2, \mathbf{t}^3)$ is the potential part.

We also note that the following assertion [132] is true in the exact formulation, i.e., before passing to the gradient expansion. Variables that allow the 'electric' interpretation do not generate a Lagrangian analog for an object taking values in the quotient space $\mathrm{SU}(3)/(\mathrm{U}(1) \times \mathrm{U}(1))$; instead, they give rise to an expression based on Kirillov's forms for the direct product of groups $\mathrm{SU}(2)^{\otimes 3}$. A number of proposals to apply the formalism of the Kirillov forms in the case of the quotient space $\mathrm{SU}(3)/(\mathrm{U}(1) \times \mathrm{U}(1))$ can be found in Ref. [133].

Magnetic variables in the SU(3) decomposition enter the Hamiltonian in a simpler way. For example, the Hamiltonian expanded in the derivatives of slowly changing mutually

uncorrelated 'electric' derivatives splits into three copies of the modified SU(2) Hamiltonian of 'magnetic' variables $\mathbf{m}^a$ and contains structures of the form

$$\eta\left(\mathbf{m}\left[\partial_k\mathbf{m}\times\partial_l\mathbf{m}\right]\right)^2+\lambda(\partial_k\mathbf{m})^2+\kappa\left(\frac{\left[\partial_k\mathbf{m}\times\mathbf{m}\right]_3 m_3}{1-(m_3)^2}\right)^2 \qquad (5.91)$$

for each magnetic unit vector $\mathbf{m}^a$. Here, $\eta$, $\lambda$, and $\kappa$ are the coupling constants. Although this Hamiltonian differs from the SU(2) Hamiltonian considered above owing to the presence of the last term, it retains the main properties of SU(2). The possibility of the emergence of such a term in the Hamiltonian of the system having string-like solutions has been discussed in Ref. [134].

There are more reasons to thoroughly examine the SU(3) case than the mere necessity of a detailed analysis of the dual picture or the known phenomenological considerations. An important problem [135] is the generalization of the geometrical interpretation of the Hopf invariant. In the case of the SU(3) group, the role of the target space $\mathrm{F}_1=\mathrm{SU}(2)/\mathrm{U}(1)=\mathrm{CP}^1=\mathsf{S}^2$ into which the unit vector $\mathbf{n}(x,y,z)$ maps is played by the flag space [136–139] $\mathrm{F}_2=\mathrm{SU}(3)/(\mathrm{U}(1)\times\mathrm{U}(1))$ or, as a particular case, by the complex projective space $\mathrm{CP}^2=\mathrm{SU}(3)/\mathrm{U}(2)=\mathrm{SU}(3)/(\mathrm{SU}(2)\times\mathrm{U}(1))$. The flag space $F_2$, being a homogeneous nonsymmetric compact Kähler manifold, is realized as a set of upper triangular matrices of the form

$$\begin{pmatrix}1 & w_1 & w_2\\ 0 & 1 & w_3\\ 0 & 0 & 1\end{pmatrix}. \qquad (5.92)$$

The entries of this matrix are parameterized by three complex functions $w_1$, $w_2$, $w_3$. In the case of the symmetric space $\mathrm{CP}^2$, $w_3=0$. We recall for comparison that $\mathrm{CP}^1$ is realized as the set of matrices having the form

$$\begin{pmatrix}1 & w\\ 0 & 1\end{pmatrix}$$

with $w=\tan(\vartheta/2)\exp(-\mathrm{i}\varphi)$, where $\vartheta$ and $\varphi$ are the angles of the spherical system of coordinates parameterizing the direction of the unit vector. The dimensions of the spaces $\mathrm{F}_2$ and $\mathrm{CP}^2$ are $\dim_{\mathrm{F}_2}=8-2=6$ and $\dim_{\mathrm{CP}^2}=8-4=4$. The 2-form $H=\mathrm{d}a=\left(\mathbf{n}\left[\mathrm{d}\mathbf{n}\times\mathrm{d}\mathbf{n}\right]\right)$ used for the $\mathrm{F}_1$ space is substituted here by the Kirillov 2-form in the orbital interpretation of these spaces.

One of the problems is the search for an analog of the linking magnetic lines. Such an analog may have the form of pre-images of the codimension-2 cycles. We recall that codimension is the difference between the dimensions of the ambient and embedded spaces. Generalization of the Hopf construction is obstructed by the fact that the 2-form $Q$ for the $\mathrm{F}_2$ and $\mathrm{CP}^2$ spaces satisfies the condition $\mathrm{d}\Omega=0$, i.e., is closed but *not exact* [140]. It may be said that $\Omega$ is an element of the second cohomology group of these spaces. This means that the 1-form, i.e., the analog of the gauge potential, can be *only locally* introduced in the flag space $\mathrm{F}_2$ as a Kähler manifold [136]. In other words, direct generalization [141] of expression (3.3) is possible only when neglecting the above circumstance, manifested as singularities on the spaces $\mathrm{F}_2$ and $\mathrm{CP}^2$, i.e., as the critical points [137] associated with the vanishing of the $w_i$ functions [142]. A reassuring fact pointing out the possibility of an analog of the Hopf invariant existing and, simultaneously, the difference between the $\mathrm{F}_2$ and $\mathrm{CP}^2$ spaces, is that the homotopy group $\pi_3(\mathrm{F}_2)=\mathsf{Z}$, as well as $\pi_3(\mathrm{CP}^1)=\mathsf{Z}$, is nontrivial, whereas $\pi_3(\mathrm{CP}^2)=0$. Also, it is worthwhile to note that the nontriviality of $\pi_2(\mathrm{F}_2)=\mathsf{Z}^2$ accounts for the presence of two different monopoles in the theory. It may be hoped that the use of the results from knot theory in higher-dimensional spaces [143] will help to resolve the problem being considered.

## 6. Concluding remarks

This communication has been designed to review some results of investigations into low-energy dynamics of excitations in the theory of strongly correlated electron systems and in the non-Abelian field theory. The problems of strong coupling, as well as the approach to them [144] in these systems, are in many respects analogous. The main purpose of applying the available results to chromodynamic phenomenology [145, 146] is to compare the estimated energies of static knotted configurations [23] with the mass of candidate glueball particles.

The analysis of dynamics of the spin degrees of freedom in condensed-matter systems was focused [15] on the hierarchy of ground states. We paid most attention to the results concerned with the essentially inhomogeneous states in spatially three-dimensional systems and to the phenomena associated with quasi-one-dimensional field configuration links. In this analysis, the homogeneous boundary conditions $\mathbf{n}(\infty)=(0,0,1)$ were assumed to be satisfied at spatial infinity. Whenever boundary conditions are other than homogeneous [31, 32], the expression for the Hopf invariant becomes more complicated. In what follows, this phenomenon is discussed with special reference to the results reported in Refs [31, 32, 147, 148]. Prior to this, however, the following fact deserves consideration.

The boundary conditions fixing the characteristic values of the momentum $\mathbf{c}$ and topological invariants $L$ and $Q$ are determined not only by the values of the driving parameter $\rho_0$ of the model and the external magnetic field or the rotation frequency of the system. Their physical meaning and concrete values also depend on the spatial dimensionality of the manifold on which the model is defined. In the $(3+0)$-dimensional case with free energy (3.2), Hopf invariant (3.3) is analogous to the Chern–Simons action $(k/4\pi)\int \mathrm{d}t\,\mathrm{d}^2x\,\varepsilon_{\mu\nu\lambda}a_\mu\partial_\nu a_\lambda$. This Abelian term in the action of $(2+1)$-dimensional systems describes the dependence of the contribution of the nonlinear modes to the free energy on the statistical parameter $k$. In the non-Abelian $\mathrm{SU}(N)$ case, the value of the coefficient is shifted by the group rank value: $k\to k+N$. The coefficient $k$ in the Chern–Simons action has the geometric meaning of the number of entanglements of the excitation world lines. Specifically, as semi-fermion excitations (the so-called semions) are permuted and returned to the initial positions on the plane, the world lines entangle twice and $k=2$. For fermions, the world lines are not entangled and $k=1$ [149]. In the classical bosonic limit, when $k\gg 1$, the statistical gauge field $a_\mu$ entering the Chern–Simons action decouples from the field describing particle states. At $k=2$, statistical correlations of the nonlinear modes are of an attractive character, and their greatest relative contribution to the energy at $k\sim 2$ is estimated at a few percent [150, 151], corresponding to several dozens or hundreds of degrees for the characteristic energy values $J\sim 0.1-1$ eV. Bearing in mind the relationship between the dimensionalities of the systems in their dynamical and statistical descriptions, the

$(2+1)$-dimensional case at $k=2$ with open ends of the excitation world lines is equivalent (the ends having been identified) to the compact statistical $(3+0)$-dimensional example of the Hopf link with $Q=1$.

The difference between the $(3+0)$- and $(2+1)$-dimensional situations is due to the topological difference between the **n**-field definition domains [31, 32, 147, 148]. When the statistical sum is calculated both in planar systems and in stratified systems in the static case (2.3) when they are periodic in one of the spatial variables, one of the three coordinates — the Matsubara variable — is also periodic. This implies that instead of the sphere $\mathsf{S}^3$, which is the domain of definition of the **n** field after the compactification of $\mathsf{R}^3$, we are dealing with a tree-dimensional torus, $\mathrm{T}^{2\times1}=\mathrm{S}^2\times\mathrm{S}^1$ or $\mathrm{T}^3=\mathrm{S}^1\times\mathrm{S}^1\times\mathrm{S}^1$, and the corresponding classes of maps. In this case, the meaning of the Hopf invariant proves to be enriched [31, 32, 147, 148]. The Hopf invariant for the three-dimensional torus $\mathrm{T}^3$ is defined modulo $2q$, where $q$ is the largest common divisor of numbers $\{q_1,q_2,q_3\}\in\mathsf{Z}$, interpreted as the number of skyrmions. Here, $q_i$ is the degree of the map $\mathrm{T}^2\to\mathsf{S}^2$, where $\mathrm{T}^2$ is the section of $\mathrm{T}^3$ with a fixed $i$th coordinate. The four integers $\{q_i,Q\}$, where the quantity $Q$ is defined modulo $2q$, provide a complete homotopy classification [148] of maps $\mathrm{T}^3\to\mathsf{S}^2$, with $\pi_1\bigl[\mathrm{Map}_q(\mathsf{S}^2\to\mathsf{S}^2)\bigr]=\mathsf{Z}_{2q}$ and a fixed degree of $q$ [31, 32, 147]. For the torus $\mathrm{T}^3$, the Hopf invariant is given by [47]

$$Q=\frac{1}{16\pi^2}\sum_{i=0}^{3}Q_i\,, \tag{6.1}$$

$$Q_3=\int \mathrm{d}^3x\,\varepsilon^{\mu\nu\lambda}a_\mu\,\partial_\nu a_\lambda\,, \tag{6.2}$$

$$Q_2=\int_{x_\mu=0}\mathrm{d}^2x\,\varepsilon^{\mu\nu\lambda}\partial_\nu\beta_\mu a_\lambda\,, \tag{6.3}$$

$$Q_1=\int_{x_{\mu,\nu}=0}\mathrm{d}x\,\varepsilon^{\mu\nu\lambda}(\Delta_\nu\beta_\mu\,\partial_\lambda\beta_\mu-\beta_\mu\partial_\lambda\beta_\nu)\,, \tag{6.4}$$

$$\begin{aligned}Q_0=2\pi\bigl[&n_1\beta_1+n_2\beta_2+n_3\beta_3+n_1\Delta_1(\beta_2+\beta_3)\\&+n_2\Delta_2(\beta_1+\beta_3)+n_3\Delta_3(\beta_1+\beta_2)\bigr]_{\mathbf{x}=(0,0,0)}\,.\end{aligned} \tag{6.5}$$

The following notation is used in these equations. The functions $\beta_1(y,z)$, $\beta_2(x,z)$, and $\beta_3(x,y)$ enter the definition of boundary conditions at the faces of a three-dimensional parallelepiped with sides $L_1$, $L_2$, and $L_3$ in the respective directions. For example, the boundary condition along the $x$ axis for the two-component function $z$ parameterizing the unit vector $\mathbf{n}(x,y,z)$ by the relation $\hat{n}=\mathbf{n}\boldsymbol{\sigma}=2zz^\dagger-1$ has the form $z(x=L_1,y,z)=\exp\bigl[\mathrm{i}\beta_1(y,z)\bigr]\,z(x=0,y,z)$. Similar boundary conditions along the $y$ and $z$ axes are defined with the help of functions $\beta_2(x,z)$ and $\beta_3(x,y)$. The functions $\beta_\mu$ satisfy the relations $\varepsilon^{\mu\nu\lambda}\Delta_\mu\beta_\nu=2\pi n_\lambda$ and are defined via $\exp(\mathrm{i}\beta_\mu)$, and hence $\beta_\mu\equiv\beta_\mu+2\pi$. In expression (6.5), $\Delta_\mu\beta_\nu\equiv\beta_\nu|_{x_\mu=L_\mu}-\beta_\nu|_{x_\mu=0}$ and $n_\nu$ is the integer-valued vector characterizing maps $\mathrm{T}^2\to\mathsf{S}^2$, where $\mathrm{T}^2$ is a section of $\mathrm{T}^3$ with a fixed $i$th coordinate.

The geometrical meaning of the modified Hopf invariant (6.1), an integer from the range $\{0,2q-1\}$, remains as before. It is the linking index of pre-images of two arbitrary points of the map $\mathrm{T}^3\to\mathsf{S}^2$. The cases of $\mathrm{T}^{2\times1}$ and $\mathrm{T}^3$ are characterized by physically different boundary conditions changing with parameter variations, e.g., upon an increase in the angular rotational velocity of the superfluid phase in $\mathrm{He}^3$ [31, 3]. The discussion of boundary conditions and other problems related to the effect of links of quasi-one-dimensional configurations on phenomena in field theory and condensed matter physics can be found in the works of A I Niemi, R S Ward, I M Cho, E Babaev, and other authors not cited in the present review and available from the Los-Alamos Preprint Archive.

In conclusion, I would like to express sincere thanks to L D Faddeev for many enlightening discussions and to P Fulde for discussions and comments, as well as for hospitality at the Institute for the Physics of Complex Systems, Dresden, where most of this review was written. I also acknowledge the useful and enjoyable talks about the relevant problems with A G Abanov, V I Arnol'd, V I Belyavskii, S A Brazovskii, L N Bulaevskii, V A Verbus, G E Volovik, Yu M Gal'perin, B A Dubrovin, N N Kirova, Yu V Kopaev, V E Kravtsov, E A Kuznetsov, A I Larkin, A G Litvak, V A Mironov, M I Monastyrskii, S G Ovchinnikov, A G Pogrebkov, V A Rubakov, G M Fraiman, D I Khomskii, A M Tsvelik, S Davis, S M Girvin, A Kundu, Yu Lu, N Nagaosa, S R Shenoy, H Takagi, and Y-S Wu. I am extremely grateful to all of them for helpful advice and suggestions.

The work was supported in part by the RFBR (grant 06-02-16561a) and the DSP Program 2.1.1 (grant No. 2369).

## 7. Appendix. Gain of free energy in the current state

The following chain of inequalities is used to prove inequality (3.5):

$$\begin{aligned}|L|<\|\mathbf{c}\|_6\|\mathbf{H}\|_{6/5}&\leqslant 6^{1/6}\bigl\|[\nabla\times\mathbf{c}]\bigr\|_2\|\mathbf{H}\|_{6/5}\\&\leqslant 6^{1/6}\bigl\|[\nabla\times\mathbf{c}]\bigr\|_2\|\mathbf{H}\|_1^{2/3}\|\mathbf{H}\|_2^{1/3}\\&\leqslant(32\pi^2)^{-4/3}F_{\mathbf{c}}^{1/2}F_{\mathbf{n}}^{2/3}F_{\mathbf{n}}^{1/6}=(32\pi^2)^{-4/3}F_{\mathbf{c}}^{1/2}F_{\mathbf{n}}^{5/6}\,.\end{aligned} \tag{7.1}$$

Here, $\|\mathbf{H}\|_p\equiv\bigl(\int\mathrm{d}^3x\,|\mathbf{H}|^p\bigr)^{1/p}$. We used the Hoelder inequality $\|\mathbf{fg}\|\leqslant\|\mathbf{f}\|_p\|\mathbf{g}\|_q$ with $1/p+1/q=1$ at the first and third steps. The second step under the condition $\nabla\mathbf{c}=0$ implies the Ladyzhenskaya inequality $\|\mathbf{c}\|_6\leqslant 6^{1/6}\|[\nabla\times\mathbf{c}]\|_2$ [152]. The fourth step follows after the comparison of the terms $\|[\nabla\times\mathbf{c}]\|$ and $\|\mathbf{H}\|$ with the terms $F_{\mathbf{n}}$ and $F_{\mathbf{c}}$. The last equality describes individual contributions from the **n**- and **c**-parts of the free energy to the final result. Assuming $\mathbf{a}=\mathbf{c}$ brings us back to the Vakulenko and Kapitanskii result [27] (see also Ref. [153]).

Similarly, the use of a chain of Hoelder and Ladyzhenskaya inequalities leads to

$$F_{\mathbf{n}}^{1/2}F_{\mathbf{c}}^{5/6}\geqslant(16\pi^2)^{4/3}|L'|\,.$$

The coefficient in this inequality differs from that in expression (3.5) due to the presence of the factor $1/4$ in front of the first term in the free energy $F_{\mathbf{c}}$.

## References

1. Faddeev L D, Preprint No. IAS-75-QS70 (Princeton, NJ: Institute for Advanced Study, 1975); *Lett. Math. Phys.* **1** 289 (1976)
2. Katritch V et al. *Nature* **384** 142 (1996)
3. Stasiak A, Katritch V, Kauffman L H (Eds) *Ideal Knots* (Ser. on Knots and Everything, Vol. 19) (Singapore: World Scientific, 1998); Kawauchi A *A Survey of Knot Theory* (Basel: Birkhäuser Verlag, 1996)

4. Wilczek F (Ed.) *Fractional Statistics and Anyon Superconductivity* (Singapore: World Scientific, 1990)
5. Protogenov A P *Usp. Fiz. Nauk* **162** (7) 1 (1992) [*Sov. Phys. Usp.* **35** 535 (1992)]
6. Dagotto E *Rev. Mod. Phys.* **66** 763 (1994)
7. Brenig W *Phys. Rep.* **251** 153 (1995)
8. Tsuei C C, Kirtley J R *Rev. Mod. Phys.* **72** 969 (2000)
9. Lee P A, Nagaosa N, Wen X-G *Rev. Mod. Phys.* **78** 17 (2006); cond-mat/0410445
10. Babaev E, Faddeev L D, Niemi A J *Phys. Rev. B* **65** 100512 (2002)
11. Kugel K I, Pogosov W V, Rakhmanov A L *Physica C* **339** 10 (2000)
12. Mel'nikov A S et al., cond-mat/0001186
13. Belyavskii V I, Kopaev Yu V *Zh. Eksp. Teor. Fiz.* **127** 45 (2005) [*JETP* **100** 39 (2005)]
14. Belyavsky V I, Kopaev Yu V, Smirnov M Yu *Zh. Eksp. Teor. Fiz.* **128** 525 (2005) [*JETP* **101** 452 (2005)]
15. Isaev L S, Protogenov A P *Zh. Eksp. Teor. Fiz.* **123** 1297 (2003) [*JETP* **96** 1140 (2003)]
16. Volovik G E, Gor'kov L P *Zh. Eksp. Teor. Fiz.* **88** 1412 (1985) [*Sov. Phys. JETP* **61** 843 (1985)]
17. Mineev V P, Samokhin K V *Zh. Eksp. Teor. Fiz.* **105** 747 (1994) [*JETP* **78** 401 (1994)]
18. Mermin N D, Ho T-L *Phys. Rev. Lett.* **36** 594 (1976)
19. Anderson P W *Phys. Rev. Lett.* **96** 017001 (2006)
20. Belyavskii V I, Kopaev Yu V *Usp. Fiz. Nauk* **176** 457 (2006) [*Phys. Usp.* **49** 441 (2006)]
21. Ioffe L B, Wiegmann P B *Phys. Rev. Lett.* **65** 653 (1990)
22. Isaev L S, Protogenov A P *Phys. Rev. B* **69** 012401 (2004)
23. Faddeev L, Niemi A J *Nature* **387** 58 (1997)
24. Gladikowski J, Hellmund M *Phys. Rev. D* **56** 5194 (1997)
25. Battye R A, Sutcliffe P M *Phys. Rev. Lett.* **81** 4798 (1998)
26. Hietarinta J, Salo P *Phys. Lett. B* **451** 60 (1999)
27. Vakulenko A F, Kapitanskii L V *Dokl. Akad. Nauk SSSR* **246** 840 (1979) [*Sov. Phys. Dokl.* **24** 433 (1979)]
28. Kundu A, Rybakov Yu P *J. Phys. A: Math. Gen.* **15** 269 (1982)
29. Ward R S *Nonlinearity* **12** 241 (1999); hep-th/9811176
30. Derrick G H *J. Math. Phys.* **5** 1252 (1964)
31. Ruutu V M H et al. *Pis'ma Zh. Eksp. Teor. Fiz.* **60** 659 (1994) [*JETP Lett.* **60** 671 (1994)]
32. Makhlin Yu G, Misirpashaev T Sh *Pis'ma Zh. Eksp. Teor. Fiz.* **61** 48 (1995) [*JETP Lett.* **61** 49 (1995)]
33. Lin F, Yang Y *Commun. Math. Phys.* **249** 273 (2004)
34. Atiyah M *The Geometry and Physics of Knots* (Cambridge: Cambridge Univ. Press, 1990)
35. Sossinsky A *Knots: Mathematics with a Twist* (Cambridge: Harvard Univ. Press, 2002)
36. The KnotPlot site, http://www.pims.math.ca/knotplot/
37. Ropers knots page, http://www.realknots.com/
38. Mathematical knots, http://www.cs.ubc.ca/nest/imager/contributions/scharein/knot-theory/
39. The knot theory MA3F2 page, http://www.maths.warwick.ac.uk/~bjs/MA3F2-page.html
40. Trefoil knot pages, http://www.jcu.edu/math/ictcm99/animations/knot.htm; http://www.unca.edu/~mcmcclur/java/LiveMathematica/trefoil.html
41. Knots, links, braids, http://www.win.tue.nl/~aeb/at/algtop-5.html
42. Knots and surfaces, http://www.ai.sri.com/~goldwate/math/knots/
43. Abanov A G, Wiegmann P B *J. High Energy Phys.* (JHEP10) 030 (2001); hep-th/0105213
44. Arnold V I, Khesin B A *Topological Methods in Hydrodynamics* (Applied Mathematical Sciences, Vol. 125) (New York: Springer-Verlag, 1998) Ch. 3
45. Moffatt H K *J. Fluid Mech.* **35** 117 (1969)
46. Gordin V A, Petviashvili V I *Zh. Eksp. Teor. Fiz.* **95** 1711 (1989) [*Sov. Phys. JETP* **68** 988 (1989)]
47. Zakharov V E, Kuznetsov E A *Usp. Fiz. Nauk* **167** 1137 (1997) [*Phys. Usp.* **40** 1087 (1997)]
48. Read N, Green D *Phys. Rev. B* **61** 10267 (2000)
49. Kamchatnov A M *Zh. Eksp. Teor. Fiz.* **82** 117 (1982) [*Sov. Phys. JETP* **55** 69 (1982)]
50. Larkin A I, Ovchinnikov Yu N *Zh. Eksp. Teor. Fiz.* **47** 1136 (1964) [*Sov. Phys. JETP* **20** 762 (1965)]
51. Fulde P, Ferrell R A *Phys. Rev.* **135** A550 (1964)
52. Buzdin A I, Kachkachi H *Phys. Lett. A* **225** 341 (1997)
53. Houzet M, Buzdin A *Europhys. Lett.* **50** 375 (2000)
54. Kuznetsov E A, Mikhailov A V *Phys. Lett. A* **77** 37 (1980)
55. Kohsaka Y et al. *Phys. Rev. Lett.* **93** 097004 (2004)
56. Kohsaka Y et al. *Physica C* **388 – 389** 283 (2003)
57. Polyakov A M *Zh. Eksp. Teor. Fiz.* **68** 1975 (1975) [*Sov. Phys. JETP* **41** 988 (1975)]
58. Niemi A J *Phys. Rev. D* **67** 106004 (2003)
59. van Baal P *Nucl. Phys. B: Proc. Suppl.* **108** 3 (2002); hep-th/0109148
60. Volkov B A et al. *Zh. Eksp. Teor. Fiz.* **81** 729 (1981) [*Sov. Phys. JETP* **54** 391 (1981)]
61. Volkov B A et al. *Zh. Eksp. Teor. Fiz.* **81** 1904 (1981) [*Sov. Phys. JETP* **54** 1008 (1981)]
62. Kotliar G *Phys. Rev. B* **37** 3664 (1988)
63. Affleck I, Marston J B *Phys. Rev. B* **37** 3774 (1988); Marston J B, Affleck I *Phys. Rev. B* **39** 11538 (1989)
64. Nersesyan A, Luther A, Preprint FTT-9 (Tbilisi: Institute of Physics, 1988)
65. Nersesyan A A, Vachnadze G E *J. Low Temp. Phys.* **77** 293 (1989)
66. Nersesyan A A, Japaridze G I, Kimeridze I G *J. Phys.: Condens. Matter* **3** 3353 (1991)
67. Hsu T C, Marston J B, Affleck I *Phys. Rev. B* **43** 2866 (1991)
68. Halperin B I, Rice T, in *Solid State Physics* Vol. 21 (Eds F Seitz, D Turnbull, H Ehrenreich) (New York: Academic Press, 1968) Ch. 1, p. 115
69. Schulz H J *Phys. Rev. B* **39** 2940 (1989)
70. Varma C M *Phys. Rev. Lett.* **83** 3538 (1999)
71. Varma C M *Phys. Rev. B* **55** 14554 (1997)
72. Wen X-G, Lee P A *Phys. Rev. Lett.* **76** 503 (1996)
73. Lee P A et al. *Phys. Rev. B* **57** 6003 (1998)
74. Nayak C *Phys. Rev. B* **62** 4880 (2000)
75. Chakravarty S et al. *Phys. Rev. B* **63** 094503 (2001)
76. Volkov B A, Gorbatsevich A A, Kopaev Yu V *Zh. Eksp. Teor. Fiz.* **86** 1870 (1984) [*Sov. Phys. JETP* **59** 1087 (1984)]
77. Volkov B A, Ginzburg V L, Kopaev Yu V *Pis'ma Zh. Eksp. Teor. Fiz.* **27** 221 (1978) [*JETP Lett.* **27** 206 (1978)]
78. Dubovik V M, Tosunyan L A *Fiz. Elem. Chastits At. Yadra* **14** 1193 (1983) [*Sov. J. Part. Nucl.* **14** 504 (1983)]
79. Dubovik V M, Tugushev V V *Phys. Rep.* **187** 145 (1990)
80. Miller M A *Usp. Fiz Nauk* **142** 147 (1984) [*Sov. Phys. Usp.* **27** 69 (1984)]; *Izv. Vyssh. Uchebn. Zaved. Radiofiz.* **29** 991 (1986)
81. Ginzburg V L et al. *Solid State Commun.* **50** 339 (1984)
82. Landau L D, Lifshitz E M *Elektrodinamika Sploshnykh Sred* (Electrodynamics of Continuous Media) (Moscow: Nauka, 1982) p. 249 [Translated into English (Oxford: Pergamon Press, 1984)]
83. Liu W V, Wilczek F *Phys. Rev. Lett.* **90** 047002 (2003)
84. Adler R J *The Geometry of Random Fields* (Chichester: J. Wiley, 1981)
85. Worsley K J *Chance* **9** 27 (1996)
86. Schmalian J "Are there gels in the quantum world?", Talk at *Aspen Intern. Workshop: Frontiers in Correlated Matter, Aspen, CO, USA, 5–8 August 2004*; http://frontiers.physics.rutgers.edu/qcrit3_files/schmallvision.pdf
87. Metzler R et al. *Phys. Rev. Lett.* **88** 188101 (2002); cond-mat/0110266
88. Gantmakher V F *Elektrony v Neuporyadochennykh Sredakh* (Electrons in Disordered Media) (Moscow: Fizmatlit, 2003) p. 160
89. Emery V J, Kivelson S A *Nature* **374** 434 (1995)
90. Mihailovic D, Kabanov V V, Müller K A *Europhys. Lett.* **57** 254 (2002)
91. Tallon J L et al. *Phys. Rev. B* **51** R12911 (1995)
92. Tallon J L et al. *Phys. Rev. Lett.* **79** 5294 (1997)
93. Boebinger G S et al. *Phys. Rev. Lett.* **77** 5417 (1996)
94. Faddeev L, Niemi A J *Phys. Rev. Lett.* **82** 1624 (1999); *Phys. Lett. B* **449** 214; **464** 90 (1999)
95. Cho Y M *Phys. Rev. D* **21** 1080 (1980); **23** 2415 (1981); **62** 074009 (2000); *Phys. Rev. Lett.* **44** 1115 (1980)
96. Cho Y M *Phys. Rev. Lett.* **46** 302 (1981)
97. Wu T T, Yang C N, in *Properties of Matter Under Unusual Conditions; in Honor of Edward Teller's 60th Birthday* (Eds H Mark, S Fernbach) (New York: Interscience Publ., 1969) p. 349
98. De Alfaro V, Fubini S, Furlan G *Phys. Lett. B* **65** 163 (1976)

99. De Alfaro V, Fubini S, Furlan G *Phys. Lett. B* **72** 203 (1977)
100. Jacobs L, Rebbi C *Phys. Rev. D* **18** 1137 (1978)
101. Protogenov A P *Phys. Lett. B* **87** 80 (1979)
102. Protogenov A P *Phys. Lett. B* **67** 62 (1977)
103. Witten E *Phys. Rev. Lett.* **38** 121 (1977)
104. 't Hooft G *Nucl. Phys. B* **153** 141 (1979); **190** 455 (1981)
105. Polyakov A M *Nucl. Phys. B* **120** 429 (1977)
106. Langmann E, Niemi A J *Phys. Lett. B* **463** 252 (1999); hep-th/9905147
107. Bae W S, Cho Y M, Kimm S W *Phys. Rev. D* **65** 025005 (2002); hep-th/0105163
108. Shabanov S V *Phys. Lett. B* **463** 263 (1999); hep-th/9907182; hep-th/0004135
109. Gies H *Phys. Rev. D* **63** 125023 (2001)
110. Belavin A A et al. *Phys. Lett. B* **59** 85 (1975)
111. 't Hooft G *Phys. Rev. D* **14** 3432 (1976)
112. Isaev L S, Protogenov A P, in *Proc. of Intern. Workshop Nonlinear Physics*: *Theory and Experiment. III, Lecce, Italy, 2004*
113. Witten E *Phys. Lett. B* **117** 324 (1982)
114. van Baal P, Wipf A *Phys. Lett. B* **515** 181 (2001); hep-th/0105141
115. Dittmann L, Heinzl T, Wipf A *Nucl. Phys. B*: *Proc. Suppl.* **106 – 107** 649 (2002); hep-lat/0110026
116. Jackiw R, Nair V P, Pi S-Y *Phys. Rev. D* **62** 085018 (2000); hep-th/0004084
117. Cho Y M, Lee H, Pak D G, hep-th/9905215
118. Witten E *Commun. Math. Phys.* **121** 351 (1989)
119. Hikami K, Kirillov A N *Phys. Lett. B* **575** 343 (2003); hep-th/0308152
120. Ward R S, hep-th/0108082
121. Skyrme T H R *Proc. R. Soc. London Ser. A* **260** 127 (1961)
122. Skyrme T H R *Nucl. Phys.* **31** 556 (1962)
123. Atiyah M F, Manton N S *Phys. Lett. B* **222** 438 (1989)
124. Manton N, Sutcliffe P *Topological Solitons* (Cambridge: Cambridge Univ. Press, 2004)
125. Manton N S *Commun. Math. Phys.* **111** 469 (1987)
126. Ward R S *Phys. Rev. D* **70** 061701 (2004); hep-th/0407245
127. 't Hooft G (unpublished)
128. Ward R S *Nonlinearity* **14** 1543 (2001)
129. Jackiw R, Nohl C, Rebbi C *Phys. Rev. D* **15** 1642 (1977)
130. Atiyah M F, Manton N S *Commun. Math. Phys.* **153** 391 (1993)
131. Faddeev L, Niemi A J *Phys. Lett. B* **525** 195 (2002); hep-th/0101078
132. Bolokhov T A, Faddeev L D *Teor. Mat. Fiz.* **139** 276 (2004) [*Theor. Math. Phys.* **139** 679 (2004)]
133. Faddeev L, Niemi A J *Phys. Lett. B* **449** 214; **464** 90 (1999); hep-th/9907180
134. Nasir S, Niemi A J, hep-th/0106009
135. Faddeev L *Philos. Trans. R. Soc. London Ser. A* **359** 1399 (2001)
136. Kondo K-I, Taira Y *Prog. Theor. Phys.* **104** 1189 (2000); hep-th/9911242
137. Picken R F *J. Math. Phys.* **31** 616 (1990)
138. Perelomov A M *Phys. Rep.* **146** 135 (1987)
139. Boya L J, Perelomov A M, Santander M *J. Math. Phys.* **42** 5130 (2001)
140. Karabali D, Nair V P, Randjbar-Daemi S, hep-th/0407007
141. Shabanov S V *J. Math. Phys.* **43** 4127 (2002); hep-th/0202146
142. Atiyah M, Witten E *Adv. Theor. Math. Phys.* **6** 1 (2003); hep-th/0107177
143. Ranicki A *High-dimensional Knot Theory. Algebraic Surgery in Codimension 2* (New York: Springer, 1998)
144. Bär O, Imboden M, Wiese U-J *Nucl. Phys. B* **686** 347 (2004); cond-mat/0310353
145. Buniy R V, Kephart T W *Phys. Lett. B* **576** 127 (2003)
146. Buniy R V, Kephart T W *Int. J. Mod. Phys. A* **20** 1252 (2005); hep-ph/0408025
147. Abanov A G, personal communication
148. Pontrjagin L *Rec. Math. Moscou* (9(51)) 331 (1941)
149. Polyakov A M *Mod. Phys. Lett. A* **3** 325 (1988)
150. Abramyan L A, Protogenov A P, Verbus V A *Pis'ma Zh. Eksp. Teor. Fiz.* **69** 839 (1999) [*JETP Lett.* **69** 887 (1999)]
151. Protogenov A P *Pis'ma Zh. Eksp. Teor. Fiz.* **73** 292 (2001) [*JETP Lett.* **73** 255 (2001)]
152. Ladyzhenskaya O A *The Mathematical Theory of Viscous Incompressible Flow* 2nd ed. (New York: Gordon and Breach, 1969)
153. Rybakov Yu P *Vestn. Ross. Univ. Druzhby Narodov Ser. Mat.* **2** (2) 35 (1995)